Volume 1 | Number 1 | Jan 2013 | Pages 1–100

ChemComm

Chemical Communications
www.rsc.org/chemcomm

ROYAL SOCIETY
OF CHEMISTRY

This is an *Accepted Manuscript*, which has been through the Royal Society of Chemistry peer review process and has been accepted for publication.

Accepted Manuscripts are published online shortly after acceptance, before technical editing, formatting and proof reading. Using this free service, authors can make their results available to the community, in citable form, before we publish the edited article. We will replace this *Accepted Manuscript* with the edited and formatted *Advance Article* as soon as it is available.

You can find more information about *Accepted Manuscripts* in the **Information for Authors**.

Please note that technical editing may introduce minor changes to the text and/or graphics, which may alter content. The journal's standard **Terms & Conditions** and the **Ethical guidelines** still apply. In no event shall the Royal Society of Chemistry be held responsible for any errors or omissions in this *Accepted Manuscript* or any consequences arising from the use of any information it contains.

ROYAL SOCIETY
OF CHEMISTRY

www.rsc.org/chemcomm

Chemical Communications

ARTICLE

Lanthanide-based luminescent biolabelling

Mohamadou Sy,[a] Aline Nonat,[a] Niko Hildebrandt,[b] and Loïc J. Charbonnière[a]*

Luminescent lanthanide complexes display unrivalled spectroscopic properties, which place them in a special category in the luminescent toolbox. Their long-lived line-like emission spectra are the cornerstones of numerous analytical applications ranging from ultrasensitive homogeneous fluoroimmunoassays to the study of molecular interactions in living cells with multiplexed microscopy. However, working such minor miracles is the results of years of synthetic efforts and spectroscopic studies to understand and gather all the necessary requirements for the labels to be efficient. This feature article intends to survey these criteria and to discuss some of the most important examples reported in the literature, before explaining in details some of the applications of luminescent lanthanide labels to bioanalysis and luminescence microscopy. Finally, the emphasis will be put on some recent applications that hold great potential for future biosensing.

1. Introduction

Revealing the presence of a biomarker in a biological fluid may sometimes appear more complicated than finding a needle in a haystack. Blood, urine, faeces or saliva are composed of millions of different molecules, among which the one of importance may only be present at an infinitesimal proportion. Although the price and user-friendliness could be non-negligible, the power of an analytical tool in this search for the tiniest amounts is principally governed by two main criteria: sensitivity and selectivity.

In bioanalytical applications, selectivity is often obtained by strong and specific biological interactions, such as the biotin-streptavidin pairing or the recognition of an antigen by an antibody. The detection of the analyte is then obtained by a specific response accompanying the recognition event. If the response may be directly monitored by a spectroscopic means (*e.g.*, absorption, circularly polarized light, fluorescence, electrochemistry), it is most often obtained by the introduction of an exogenous marker that provides a typical signature associated to the recognition event. The marker or label aims at providing the sensitivity to the analysis. In the 1960's, very high sensitivity was first obtained by the development of radioimmunoassays, following the pioneering work on ^{131}I labeled insulin.[1] But the difficulties associated to the handling of radioisotopes (*e.g.*, expensive equipment, official licenses, waste disposal) prompted the search for alternative labels and luminescent ones rapidly appeared very

promising and perfectly competitive in terms of sensitivity, costs, and user-friendliness.[2] Nevertheless, fluorescent labels, should they be simple organic molecules[3] or sophisticated genetically encoded proteins,[4] still suffer from few drawbacks. Upon optical excitation, the promotion of electrons in antibonding orbitals may result in undesired photochemical reactions, leading to the destruction of the dye, i.e. photobleaching, especially upon long exposure times, as it may be the case for microscopy imaging.[5] In complex biological fluids, the fluorescent signal of the label can become blurred by the spurious fluorescent signals arising from autofluorescence of the endogenous sample components. Finally, the energy difference between the maxima of absorption and emission of the fluorescent compounds, the so-called effective Stokes' shift, does not exceed much more than 1000 cm^{-1}, so that the absorption and emission spectra substantially overlap. This overlap results in the need for an efficient filtering of the excitation and emission detection channels to avoid spectral crosstalk between the channels, resulting in a concomitant loss of signal intensity.

Thanks to their exceptional luminescent properties,[6,7] lanthanide (Ln) labels are able to bypass all of these negative issues and they can afford ultrahigh sensitivity in bioanalytical applications, even for homogeneous assays in whole blood.[8] This feature article aims at providing the basic principles of luminescent lanthanide complexes, how they can be introduced as labels on biological compounds and used in bioanalytical detection or for luminescence microscopy. Although we will sometimes refer to Ln based nanoparticles, especially when photon upconverting properties will be discussed, the focus will be essentially made on discrete molecular complexes and those readers interested in Ln based (nano)-materials should refer to the corresponding literature.[9-11] In a last part, we will put the emphasis on some recent trends in luminescent lanthanide labels and their perspectives for bioanalytical applications.

[a.] *Laboratoire d'Ingénierie Moléculaire Appliquée à l'Analyse, IPHC, UMR 7178 CNRS, Université de Strasbourg, ECPM, Bât R1N0, 25 rue Becquerel, 67087 Strasbourg Cedex, France. E-mail : l.charbonn@unistra.fr*
[b.] *NanoBioPhotonics, Institut d'Electronique Fondamentale, Université Paris-Saclay, Université Paris-Sud, CNRS, Orsay, France.*
† Footnotes relating to the title and/or authors should appear here.
Electronic Supplementary Information (ESI) available: [details of any supplementary information available should be included here]. See DOI: 10.1039/x0xx00000x

2. Lanthanide complexes as luminescent labels: general properties.

2.1. General properties of luminescent lanthanide cations. In aqueous solutions, the +III oxidation state is the most stable for all lanthanide cations. The optical properties arise from the $[Xe]4f^n$ configurations (n = 0 to 14 from La to Lu). Considering that the radial extension of 4f orbitals is smaller than that of the filled $5s^2$ and $5p^6$ orbitals of Ln^{3+}, the electrons involved in the transitions are shielded from the environment (solvent molecules, ligands, anions) resulting in very weak perturbations of the transitions by the ligand field and characteristic emission spectra for each Ln^{3+} cation, *i.e.* elemental spectral signatures. Although weak (few tenths of cm^{-1}), these perturbations can be informative and used, in the case of Eu^{3+}, to correlate the energy of the $^5D_0 \rightarrow {}^7F_0$ transition to the number of coordinating atoms and to their effects on the ligand field expressed in terms of nephelauxetic parameters.[12]

The optical properties of Ln^{3+} cations are associated to electronic transitions within the 4f orbitals which are governed by the selection rules on the spin (S), orbital (L) and total (J) angular momenta quantum numbers.[13] The magnetic dipole transitions are allowed, but weak, whereas the electric dipole transitions are forbidden by the Laporte and sometimes spin multiplicity rules, but can be relaxed by symmetry considerations, being also weak. It results that the absorption cross sections of f-f electronic transitions of Ln^{3+} have very low extinction coefficients (few units $M^{-1}cm^{-1}$ in the best cases) and the direct excitation of the cations through these transitions is difficult. However, in 1942, Weissman observed that the photoluminescence (PL) of Eu cations could be largely increased in the presence of some organic aromatic ligands.[14] Interestingly, the excitation of Eu was observed at wavelengths were the cation does not absorb and it was concluded that the excitation was a multistep process with absorption of the ligands, energy transfer to Eu followed by its emission. This was the basis of what would be later called the "antenna effect",[15] in which heteroaromatic ligands are designed to coordinate to the Ln^{3+} emitters, providing very large absorption through the aromatic moieties. Since then, the antenna effect has been extended to almost all Ln^{3+} cations being visible or near infrared (NIR) emitters,[16,17] and for some of them (Eu and Tb), some empirical rules have been developed to rationalise the matching of the ligand centred excited-state levels with the targeted luminescent Ln cation.[18,19] Additionally, the antenna effect has another advantage. While the excitation of the ligand is generally performed in the UV to blue spectral region, the emission is observed in the visible or NIR domain and the effective Stokes' shift is large, decreasing the need for efficient filtering between the excitation and emission channels.
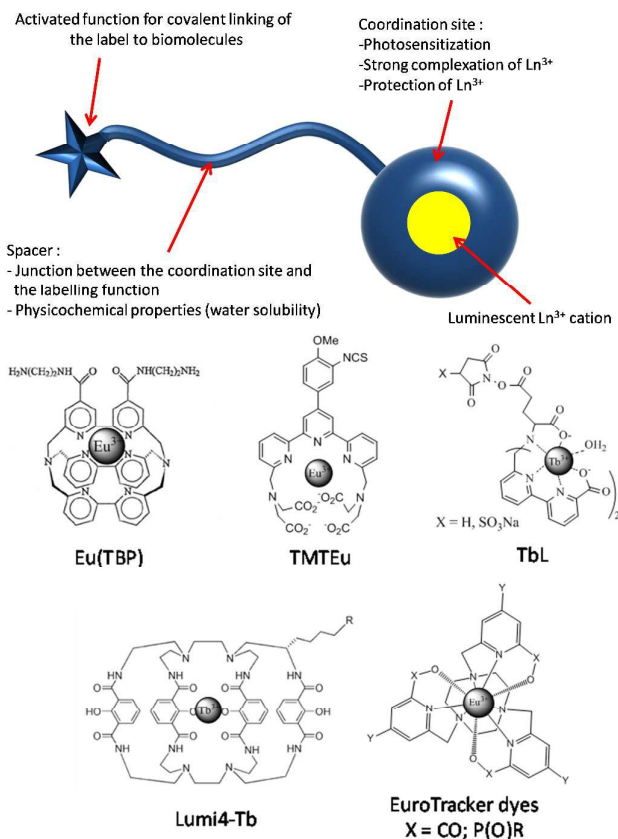
Scheme 1. Schematic representation of a luminescent lanthanide label and its basic constituents (top) and representative examples from the literature (bottom, see text).[30,32,33,39,40]

When the impact of selection rules is deleterious for the absorption properties, it is also at the origin of one of the most alluring properties of Ln PL. Once a Ln-centred excited state has been reached, by direct excitation or via the antenna effect, the rules for radiative de-excitation are the same and the probability is weak. As a consequence, the excited-state lifetimes of Ln can be extremely long, up to few milliseconds for visible Eu and Tb emitters and even tens of microseconds for NIR emitting Yb complexes.[20] Considering that the excited-state lifetimes of fluorescent compounds is of the order of few nanoseconds, this property opens an avenue for a very sensitive detection of Ln emission based on time-resolved or time-gated PL.[21,22]

Finally, a last important point to consider in the design of luminescent Ln labels is the crucial role played by OH, NH and CH oscillators in the possible quenching of the Ln emission. In the late 1970s, Horrocks and co-workers demonstrated that the PL lifetime of Eu and Tb complexes was directly related to the number of O-H oscillators in the first coordinating sphere of the cations.[23] By comparing lifetimes measured in H_2O and D_2O, they derived empirical rules that allowed to determine the number of water molecules in the first coordination sphere. This pioneering work was followed by numerous

others, including the influence of other oscillators (NH, amide NH, CH) and outer-sphere contributions[24,25] as well as other Ln^{3+} cations (Dy, Sm),[26] among which some NIR emitters (Yb and Nd).[24,27,28]

Another consequence of the shielding of 4f electrons and the very poor orbital overlap with the ligands is that the chemical bonds with the coordinated atoms is essentially electrostatic in nature and the Ln^{3+} cations do not present stereo-electronic preferences. The coordination of the ligands will be essentially guided by a subtle balance between the strength of the electrostatic interactions between Ln^{3+} and the ligands and steric repulsion interactions between the ligands around the cation. In aqueous solutions, the coordination numbers (CN) are generally ranging from 8, especially for the smaller cations of the series (Lu), to 10.

2.2. Lanthanide labels. In addition to fulfilling the first coordination sphere of the lanthanide and a good matching of its singlet and triplet energy levels with those of the targeted cation, an efficient Ln label must also exhibit a strong coordination to the Ln cation affording high thermodynamic and kinetic stabilities. There are essentially two strategies to reach this stabilization. The first is to use highly pre-organized ligands featuring macrocyles such as triazacyclononane (TACN,[29] see also the Eurotracker family,[30] Scheme 1) or 1,4,7,10-tetraazacyclododecane (Cyclen),[31] or macrobi- and tricycles (see resp. [Eu(TBP)][32] or Lumi4-Tb[33] for examples, Scheme 1). The second strategy is to provide numerous negatively charged functions such as carboxylates, phosphinates or phosphonates. It should here be mentioned that complexes featuring phosphonate functions are among the most thermodynamically stable complexes with Ln cations.[31,34,35] A third alternative strategy was developed by Piguet and Bünzli, who obtained very stable Ln labels thanks to supramolecular chemistry. They demonstrated the assembly of three ligand strands around two Ln cations in a dinuclear triple helix to obtain extremely stable water soluble edifices.[36]

In summary, the main pre-requisites to build a ligand that will afford an efficient Ln label are:

- High absorption coefficient.
- Fine tuning of the singlet and triplet energy levels depending on the targeted Ln cation.
- Good shielding of the Ln^{3+} cation by the ligand (CN = 8 to 10).
- High thermodynamic and kinetic stabilities.
- Compatible physicochemical properties with biological media.
- An activated labelling function.

The question of physicochemical biocompatibility is mainly a question of water solubility. If it is not an absolute condition in the activated form of the Ln label, water solubility is of course mandatory to avoid too much changes in the physicochemical properties of the labelled biological compounds. Nevertheless, water solubility is not mandatory in

the activated form, providing the label is soluble enough in highly polar solvents (DMSO, DMF). It may even be an advantage for the long term storage of the activated label in solution, preserving the activated function from hydrolysis.

Scheme 1 depicts a basic representation of a luminescent lanthanide label and its different constituents, together with some representative examples. The Eu(TBP) complex was one of the very first Ln labels to be developed and used in bioassays.[37] Originating from the work of Lehn and coworkers on the cryptand compounds,[32] the structure of the ligand was designed to accommodate three bipyridine units for an efficient photosensitization of europium, ensuring a very high stability thanks to its microbicyclic structure. Soon after, a non-macrocyclic Eu complex, TMTEu, based on a terpyridine scaffold was patented by Eastman Kodak Company[38] and reported in the literature.[39] If the complex was highly luminescent, the labelling was a two-step procedure necessitating the coupling of the biomolecule with the activated ligand prior to complexation of Eu. Interestingly, much of the initial work on Ln-based labels was directed against Eu complexes, in part because the PL spectrum of Eu is generally dominated by the narrow $^5D_0 \rightarrow {}^7F_1 + {}^7F_2$ transitions in the red region around 580-620 nm.[40] However, the interest to play with more than one emission band, especially for multiplexing applications (see below), led to a stronger use of Tb and its four intense narrow emission bands spanning the visible region ($^5D_0 \rightarrow {}^7F_J$ with J = 6 to 3 at *ca.* 485, 545, 580 and 620 nm). In 2004, we reported the development of one of the first highly luminescent Tb labels (TbL, Scheme 1).[41] Despite the presence of one inner sphere water molecule, the complex displayed an interesting 31% PL quantum yield in water and a NHS ester that was used for biolabelling of streptavidin allowing for the first evidences of Förster resonance energy transfer (FRET) experiments with quantum dots.[42] In 2011, Raymond and coworkers reported on the development of a highly luminescent Tb complex based on a macrotricyclic chelate bearing four 2-hydroxyisophthalimide chromophoric units, now commercialized as Lumi4-Tb.[33] Thanks to the four absorbing units, they reported values superior to 10 000 $M^{-1}cm^{-1}$ for the brightness (the brightness represent the product of the extinction coefficient at the excitation wavelength and the PL quantum yield), and Lumi4-Tb is currently used in numerous analytical applications (*vide infra*). The latest events in the development of luminescent lanthanide labels arose from the work of Parker, Maury and coworkers, which resulted in the development of the Eurotracker dye family (Scheme 1).[30] The association of the efforts on *para*-substituted dipicolinic acids[43] and on the introduction of phosphinic acid functions,[44] gathered on a triazacyclonane scaffold, afforded the highest values of brightness ever reported for lanthanide labels climbing up to 22 000 $M^{-1}cm^{-1}$.

2.3. The labelling function. Last but not least, the covalent grafting of luminescent lanthanide labels on biological material requires the introduction of a labelling function in the design of the ligand. If the labelling can be operated in-situ, for example by activation of a carboxylate function of the ligand with reactant such as DCC or EDCI,[46] or reaction of amino[47] or aminoxy[48] containing ligands with dialdehydes, this methodology is accompanied by few drawbacks such as the possibility of cross-coupling reactions (activation of the biomolecule which reacts on itself), of activation of more than one function of the ligand, or of the decrease of the chelate stability arising from the change of carboxylate functions into amide ones. Therefore, it is preferred to provide the label with an activated function that will react with specific functions of the biomaterial to tag. The activated function can be present on the Ln label, but in some other instances, it is the activated ligand that is synthesized, the Ln cation being added only after the coupling of the ligand to the biomaterial to form the Ln label. Scheme 2 represents some of the most important classes of activated functions in existing examples of the literature.
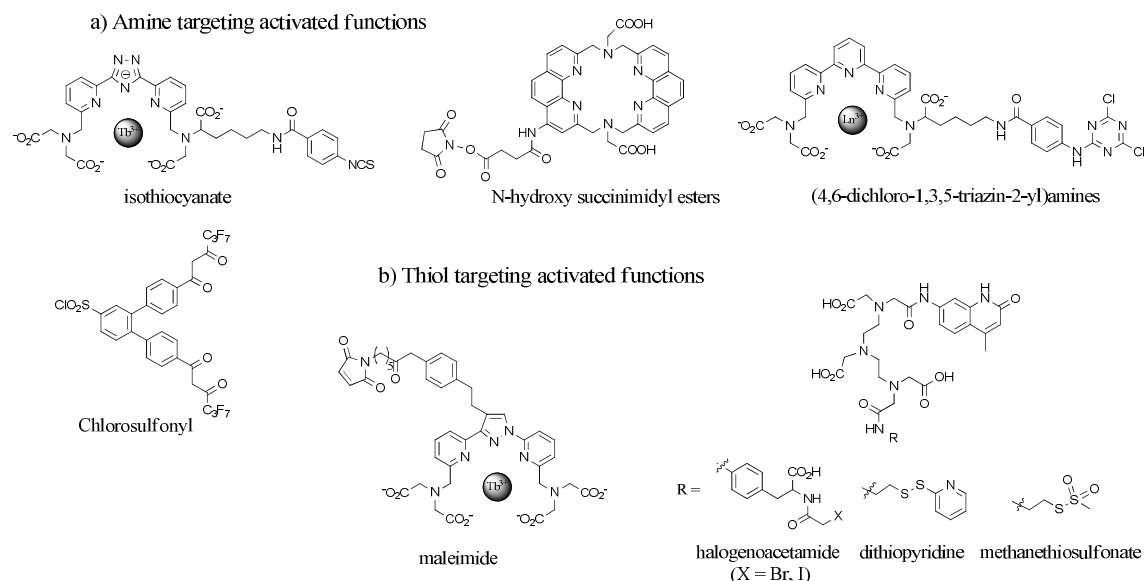
Scheme 2. Representative examples of ligands bearing amine- and thiol-targeting activated functions

The most important class of activated functions are those targeting amino residues as they are highly represented on biomolecules in the form of the N-ter function of proteins or on lysine amino acids. The isothiocyanate function has been largely developed in the labels synthesized by the group of Wallac Oy in Turku, Finland, and is generated by the reaction of an aromatic primary amine with thiophosgene.[49] It can be introduced on an appended aromatic residue (see example in Scheme 2)[50] or on an aromatic ring constitutive of the antenna.[39,51] Upon reaction with amines, the isothiocyanate forms a strong thiourea bond between the label and the biomaterial. The chlorosulfonyl function was one of the very first activated functions to be used for biolabelling by the group of Evangelista and coworkers.[52] it is generally obtained by the reaction of chlorosulfonic acid on aromatic phenyl rings[53] and reacts with amine to form sulfonamide bonds. The main problem of chlorosulfonylation are the lack of chimioselectivity (both *ortho*- and *para*-functionalization can be observed on the phenyl rings), and its strong reactivity, rendering it very sensitive in aqueous basic media. Dichlorotriazines have also been largely used as activated function.[54] They are obtained from reaction of chlorocyanuric acid with amines. Of particular interest, the reaction of chlorocyanuric acid is very particular. It can react three times with amines. The first reaction is extremely easy allowing for the introduction of a dichlorotriazine on amino containing Ln complexes, yielding to an activated function at low temperature. The second reaction with an amine is of medium reactivity, leading to the coupling with biomolecules at or near r.t. Finally, the third reaction requires heating with a third amine, thereby avoiding polysubstitution.[55] N-hydroxysuccinimidyl esters (NHS) and their more water soluble sulfonated version (Sulfo-NHS) are very attractive activated functions that react with amine to form amide functions. They are obtained from reaction of a carboxylic acid with carbodiimide (DCC, EDCI) in the presence of hydroxysuccinimide.[46a,56] An interesting particularity of NHS esters is that they resist to acidic conditions and can be introduced early in the synthesis before deprotection of acid sensitive protecting groups such as t-butyl esters (cleaved with TFA)[57] or TMSBr deprotection of phosphonic esters.[58]

ARTICLE

Thiol functions are less present in proteins, but they can be found as cysteine residues or be generated during the fragmentation of antibodies that results from the breaking of cystine bridges.[59] Therefore, they present some more specific target sites for a localized labelling of biomaterials. The most commonly used thiol targeting function is maleimide (Scheme 2),[60] which reacts through a Michael addition to form a thioether bridge. The group of Selvin has also developed a large library of other thiol directed labelling functions such as halogenoacetamides, dithiopyridines or methanthiosulfonate groups.[61]

There also exist some less common activated functions, among which one can notice some very elegant examples of phosphoramidate activated groups for the labelling of oligonucleotides developed by different groups, among which that of Hovinen and coworkers.[62]

3. Applications of Ln-based properties for improved bioanalytical applications

3.1. Time-resolved detection.

The excited-state lifetimes of Ln labels can span up to few milliseconds for Eu and Tb complexes and is generally of the order of microseconds for other Ln complexes. This is typically two to six orders of magnitude longer than conventional organic dyes (up to few tens of ns) and semiconducting nanocrystals (*ca.* 1 to 100 ns). The basic principle of time-resolved (or time-gated) detection is to implement a delay between the pulsed excitation of the sample and the acquisition of the emitted luminescent signal. This delay will allow for the vanishing of the fast fluorescence signals, arising from autofluorescence of the sample or from the presence of fluorescent compounds, or scattering of light in the instrumental set up. As these signals are removed, the remaining PL only originates from long-lived emitters, *e.g.* Ln labels,[63] and delayed acquisition offers a very large increase in the signal to noise ratio (more than three orders of magnitude)[64] associated with the presence of the Ln label.
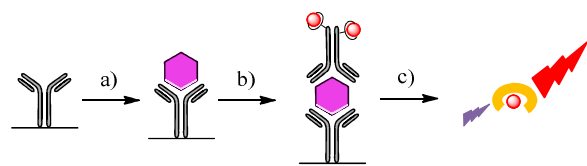

Figure 1. Principle of the DELFIA system with time-resolved (or time-gated) detection. a) Antigen fixation on a solid-supported primary antibody. b) Reaction with a Ln labelled secondary antibody. c) Rinsing and Eu PL enhancement with time-gated PL detection.[65]

The principle of time-resolved detection was largely developed by the group of Wallac Oy in the 1980th,[65] in the DELFIA® system (Dissociation Enhanced Lanthanide Fluorescence ImmunoAssay) for a highly sensitive detection of antigens. The basic principle is depicted in Figure 1. It consists in a four steps process: 1) fixation of the antigen on

a primary antibody fixed at the surface of the walls; reaction of a secondary antibody labelled with a non-luminescent Ln complex; 3) rinsing and 4) addition of an enhancing solution containing reagents that form highly luminescent Eu complexes in micelles. After excitation at 340 nm, the emitted intensity is recorded in the time-gated mode, suppressing the fluorescence of the different compounds and only the Ln PL is recorded, leading to subpicomolar detection limits in the case of Eu (0.05 pM).[65]

One of the main drawbacks of the DELFIA system is the multistep approach necessitating various fixation, washing and separation operations. These drawbacks can be eliminated by the use of luminescent lanthanide chelates within the frame of homogeneous time-resolved fluoroimmunoassays (TR-FIA) depicted in Figure 2.[66] A stock solution contains a mixture of two labelled antibodies, one labelled with a luminescent Ln complex (generally Eu or Tb), the second labelled with a fluorescent acceptor dye. These Ln/dye pairs are usually chosen for a maximum spectral overlap of the emission spectrum of the Ln energy donor and the absorption spectrum of the fluorescent energy acceptor and minimum spectral overlap of both emission spectra. When donor and acceptor are in close spatial proximity (few nm), the spectral overlap allows for FRET from the donor to the acceptor. The occurrence of FRET can be observed by the emission of the dye after excitation of the Ln.

In absence of antigen (Figure 2, top), the high dilution of the antibodies in solution (typically in the nM range) precludes the close proximity of the antibodies and hence, the energy transfer between the Ln donors and dye acceptors. Excitation of the Ln donor, generally in the 300-350 nm region, leads to emission of the Ln and in part to emission of the dye, which disappears if the acquisition is performed in the time-resolved mode with a delay of typically a few μs).
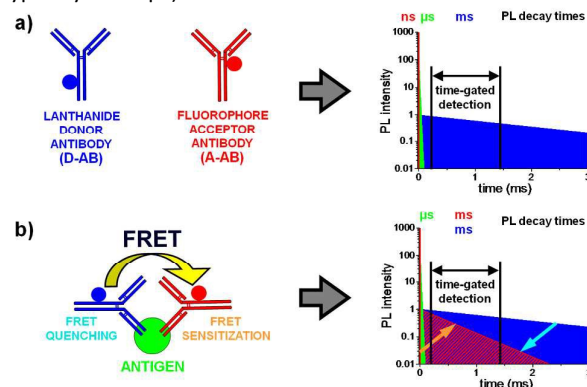

Figure 2. Principle of homogeneous time-resolved fluoroimmunoassays (TR-FIA).

Once the antigen is introduced into the solution, the immunologic reactions lead to the formation of "sandwich" like adducts of the antigen with its specific antibodies. These structures result in the close spatial proximity of the donor and acceptor molecules, now allowing for FRET to occur. Upon excitation of the Ln chelate, in addition to the

signals emitted by the Ln labels due to unreacted antibodies and that due to direct excitation of the dye comes a third signal originating from the emission of the dye after energy transfer from the Ln labels in the sandwiches. Importantly, this last process arising from a very long lived Ln donor is delayed in time and the fluorescence issued from FRET is observed with a lifetime far longer than that of the dye alone (providing the donor-acceptor distance is not to short, i.e. FRET is not too efficient).[67] In the time-resolved mode, one will observe a new emission signal at the dye emission wavelength due to FRET. This signal being proportional to the concentration of immunosandwiches formed, its quantification is a direct measure of the concentration of antigen present in solution.

In practice, the effectively measured signal is the ratio of the emission intensity of the dye over that of the Ln donor in the time-gated detection window. This ratiometric measurement has the further advantage to be independent of the concentrations of antibodies in the solution when the relative concentrations of Ln labelled and dye labelled antibodies is constant. The power of this technology essentially resides in its sensitivity for a homogeneous assay, with detection limits in the pM or fM range,[68] with multiplexed capabilities (*vide infra*), and the capacity to be transposed to other bioanalytical systems requiring high sensitivity such as PCR.[69]

3.2. Multiplexed analysis

The multiple and narrow PL bands and the long excited-state lifetimes of Ln ions can also be exploited for multiplexed biosensing, *i.e.* analysing several biological components or biological interactions from a single sample. Ln-based multiplexed analysis has been realized by three different strategies: (*i*) tuning the PL wavelength by the selection of different Ln-ions,[70-87] (*ii*) tuning the PL wavelength by using a Ln-ion as FRET donor in combination with several multi-coloured FRET acceptors,[88-112] and (*iii*) tuning the PL lifetime by using a Ln-ion as FRET donor and a Ln-ion or dye acceptor.[113,114] Both photon downshifting (commonly used PL, for which the excitation wavelength is shorter than emission wavelength) with luminescent Ln-ions (Dy^{3+}, Eu^{3+}, Sm^{3+}, Tb^{3+}) embedded in nanoparticles[70-72,75,78,80,81,83,113,114] or coordinated to supramolecular complexes[74,76,77,79,86-104,106-112] and photon upconversion (excitation wavelength is longer than emission wavelength) with luminescent Ln-ions (Dy^{3+}, Er^{3+}, Ho^{3+}, Tm^{3+}) embedded in nanoparticles[70,73,80-82,84,85,105,114] have been used for Ln-based multiplexing. The enormous potential of Ln-ions for colour multiplexing using both downshifting and upconversion is illustrated in Figure 3.

Several of the above mentioned studies were proof-of-concepts for multiplexed (multicolour) detection and did not contain any biomolecules.[70-72,76,80-82] On the other hand, many multiplexed bioanalytical applications were demonstrated, which used various biomolecules, such as

biotin/(strept)avidin,[73,92,93,95,96,98,103,104,107] nucleic acids,[73,75,89,93,95-97,104,105,111-113] peptides,[73,88-92,94,95,101,102,109] and antibodies,[73,74,78,94,95,98-101,106,108,110] for Ln-bioconjugation or developed analyte-sensitive Ln-complexes.[79,86,87]
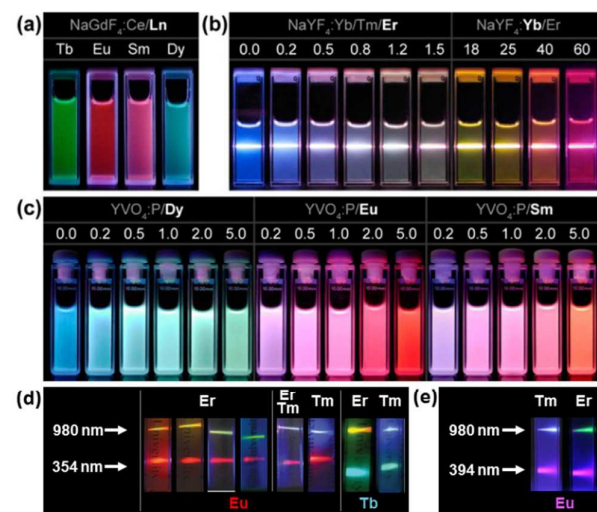

Figure 3: Variation of PL wavelengths using luminescent Ln-ions. (a) PL colours of Ln-ions embedded in NaGdF$_4$. Adapted with permission from reference 83. Copyright 2007 IOP Publishing. (b) Multicolour upconversion PL of Tm^{3+} and Er^{3+} (at varying concentration of Er^{3+} and Yb^{3+}) in NaYF$_4$ nanoparticles. Adapted with permission from reference 84. Copyright 2008 American Chemical Society. (c) Multicolour downshifting PL of Dy^{3+}, Eu^{3+}, and Sm^{3+} (at varying concentrations) in YVO$_4$ nanoparticles. Adapted with permission from reference 85. Copyright 2008 WILEY-VCH Verlag GmbH & Co. KGaA.(d) Simultaneous upconversion (top PL lines) upon 980 nm excitation (at different concentrations of Tm^{3+} and Er^{3+}) and downshifting (Eu^{3+} and Tb^{3+} PL) upon 354 nm excitation of core/shell nanocrystals composed of Yb^{3+}, Er^{3+}, and/or Tm^{3+} embedded in NaYF$_4$/NaLuF$_4$ cores and SiO$_2$ shells doped with Eu^{3+} or Tb^{3+} complexes. Adapted from reference 70. (e) Simultaneous upconversion and downshifting of NaYF$_4$:Yb/Er(Tm)/Eu nanoparticles. Adapted with permission from reference 81. Copyright 2010 Elsevier B.V.

In addition to the significant background suppression due to the long PL lifetimes of the Ln, their narrow and well separated emission bands allowed the multiplexed detection of several biologically relevant analytes and their activity (*e.g.*, enterotoxins,[75] enzymes,[79,88,102] ions,[77] proteins and other tumour markers,[74,99,100,107,108,110] nucleic acids,[89,97,104] reactive oxygen and nitrogen species,and hydrogen peroxide[79]), the monitoring of several biological interactions (*e.g.*, binding of multiple ligands to the human nuclear receptor,[101] the thyroid hormone receptor,[96] or the estrogen receptor[98]), and the development of DNA photonic wires,[111] molecular logic devices,[91,92] and molecular/spectroscopic rulers.[103,107,109] In the following paragraphs we want to highlight each of the three aforementioned multiplexing strategies (*i-iii, vide supra*) by one recent, pertinent, and representative example.

i) Multiplexing using different lanthanides: In 2015 Pershagen and Borbas developed analyte-responsive Ln-complexes that combined facile synthesis, colour-multiplexing by simple exchange of Ln-ions, and multiple analyte-specificity by exchangeable analyte-cleavable caging groups, which triggered the off-on excitation/emission of the Ln-ion (Figure 4a).[79] The authors designed Tb-, Eu-, and Gd-based probes against α-mannosidase, β-glucosidase, reactive nitrogen and oxygen

species, H_2O_2, β-galactosidase, and phosphatase with up to 90-fold on/off intensity ratio. Triplexed detection of the latter three analytes was demonstrated by using Eu and Tb probes in time-gated PL detection mode and a coumarin probe in steady-state detection mode. The differences in excitation and emission spectra (Figure 4b) allowed distinct excitation and detection of the different analyte-responsive probes with very good specificity (Figure 4c). Although only two lanthanides could be used in this study the relatively simple Ln-ion exchange (*e.g.* with Sm or Dy) and the demonstration of a parallel use of dye- and Ln-based probes should enable higher multiplexing capability in the future.
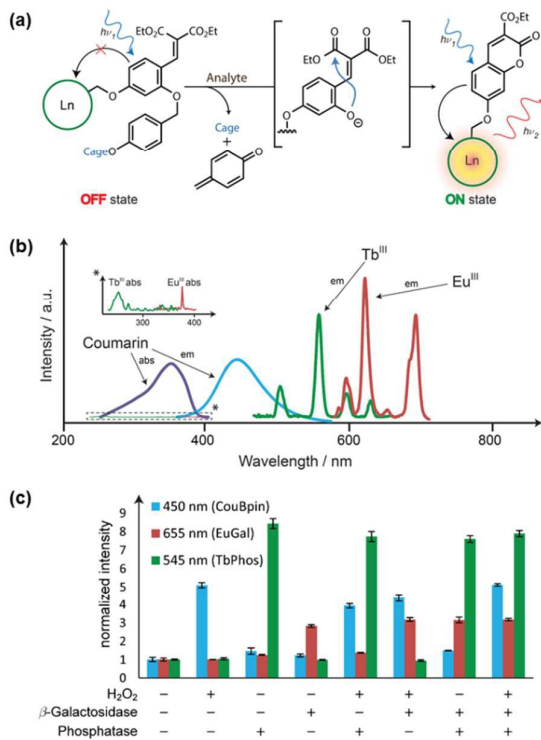

Figure 4: Triplexed analyte detection using off-on PL probes. (a) Principle of switching on the Ln PL by an analyte-specific cage group, whose detachment leads to the activation of the Ln-sensitizing antenna complex. (b) Excitation and emission spectra of off-on probes using the Ln-ions Tb^{3+} and Eu^{3+} and a coumarin dye. (c) Using the three probes from b with H_2O_2, β-galactosidase and phosphatase cage groups allowed for very specific duplexed and triplexed detection of the three analytes. Adapted with permission from reference 79. Copyright 2015 Wiley-VCH Verlag GmbH & Co. KGaA.

ii) Multiplexing using lanthanides as FRET donors: Also in 2015 Hildebrandt *et al.* demonstrated the use of FRET from a Tb donor to three different organic dye acceptors for triplexed detection of microRNA (miRNA).[97] Excitation at 337 nm led to the characteristic Tb PL spectrum, which overlapped with the absorption spectra of Cy3.5, Cy5, and Cy5.5 (Figure 5a). This spectral overlap resulted in Tb-to-dye FRET upon the hybridization/ligation-based binding of miRNA to two Tb-DNA and dye-DNA probes, which brought Tb and dye in a FRET-relevant proximity. The time-gated PL intensities of the FRET-quenched Tb donor (Figure 5c) and the FRET-sensitized dye acceptors (Figure 5d) could be measured at distinct emission wavelengths (Figure 5b) for a

quantification of the nucleic acid analytes. Both three different miRNAs (Figure 5e) and three different single-stranded DNAs (ssDNA; Figure 5f) with strong sequence homologies could be sensitively and specifically detected in a single sample and at varying concentrations between 50 and 500 pM. Addition of 5% serum to the samples did not alter the sensitivity and demonstrated a possible use of this technology for the detection of blood-circulating miRNA for clinical diagnostics. The addition of more acceptor dyes (as demonstrated for lung-cancer immunoassays)[110] may also enable higher multiplexing capability in the future.
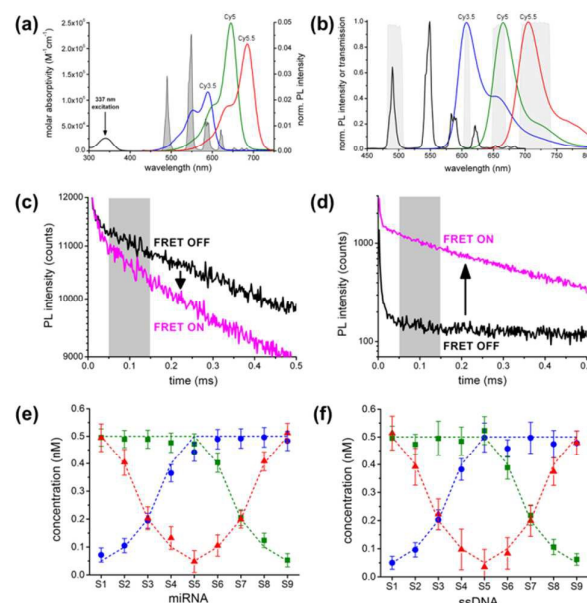

Figure 5: Triplexed miRNA sensor using Tb-to-dye FRET. (a) Absorbance spectra (left ordinate) of the Tb-donor and the acceptor dyes Cy3.5 (blue), Cy5 (green) and Cy5.5 (red). Area-normalized PL spectrum of Tb (grey in the background) is shown for visualization of donor-acceptor spectral overlap. (b) PL emission spectra of Tb (black), Cy3.5 (blue), Cy5 (green) and Cy5.5 (red). Transmission spectra of Tb-donor and dye-acceptor detection channels are show in grey in the background. (c+d) Representative PL decay curves measured in the Tb-detection channel (c) and in the Cy3.5 detection channel (d). FRET OFF/ON curves present the absence/presence of target miRNA. The grey areas represent the time-gated PL detection windows. (e+f) Varying concentrations (dotted lines indicate the known concentrations) of miRNA (e) or ssDNA (f) could be measured with high precision using multiplexed Tb-to-dye FRET. S1 to S9 represent nine different samples. Different colours represent the different miRNA targets (hsa-miR-20a-5p, -20b-5p, and -21-5p) and their ssDNA analogues, respectively. Reprinted with permission from reference 97. Copyright 2015 Wiley-VCH Verlag GmbH & Co. KGaA.

iii) Multiplexing using lanthanide luminescence lifetime: In 2014, Jin *et al.* published two studies, in which they demonstrated the use of different Ln PL decay times for multiplexed detection. For this purpose they designed Yb^{3+}/Tm^{3+} doped $NaYF_4$ upconversion nanocrystals (UCNPs) with a diameter of approximately 40 nm, for which the PL decay times were tuned by varying the Tm^{3+} concentration (and therefore Yb-Tm distance),[114] and Eu^{3+}/dye doped polystyrene beads (~15 μm), for which the PL decay times were tuned by varying the dye concentration (and therefore Eu-dye distance).[113] The variation in doping ratios could be used to tune quite precisely the PL decays of the UCNPs and the Eu-to-dye FRET microspheres (Figure 6) in the tens to hundreds of μs average decay time range. The development of appropriate fit algorithms allowed to

ARTICLE   Journal Name

efficiently distinguish five different average decay times for both approaches. The authors also developed an imaging technology (time-resolved orthogonal scanning automated microscopy: TR-OSAM) that was applied for the multiplexed detection of different microspheres (doped with the UCNPs or the Eu-dye FRET-pairs) on microscopy slides. A proof-of-concept for multiplexed biosensing was shown for the detection of four different ssDNAs that were captured by complementary ssDNAs conjugated to four different Eu-dye microspheres (with different PL decay times). The assay procedure included 1 h incubation of all the capture-DNA microspheres with the four biotinylated target DNAs, washing, 1 h incubation of that suspension with streptavidin-coated quantum dots (QDs), washing, and preparation of the final suspension on glass slides. Using the TR-OSAM technology the glass slides were then scanned and the different microspheres (and therefore the different DNAs) could be efficiently distinguished by their PL decay times. Quantification of the DNAs was possible by measuring the PL intensity of the co-labelled QDs.
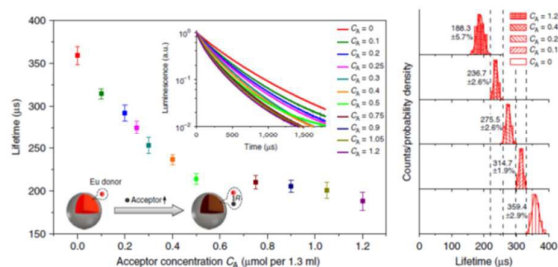

Figure 6: PL decay time tuning within FRET microspheres. Increasing concentrations of acceptor dyes led to a closer average distance to the Eu³⁺ donor and concomitant shorter PL decay times of the Eu³⁺. Among all samples, five types of microspheres gave distinct PL decay time ranges without significant overlap. These could be used for multiplexed ssDNA detection using TR-OSAM. Reprinted with permission from reference 113. Copyright 2014 Macmillan Publishers Limited.

Although the time-resolved multiplexing approach requires several incubation and washing steps, imaging of spatially separated microbeads, and an additional PL intensity marker for quantification, it could impressively demonstrate the relatively rapid, sensitive, and accurate multiplexing capabilities of different PL decay times. Further optimization of such energy transfer-tuned nano- and microparticles may lead to additional distinguishable decay times and combination with colour multiplexing can further enhance the multiplexing capability of these multiplexed Ln PL probes. As shown above, lanthanide-based PL detection provides an exceptional versatility for multiplexed biosensing. A combination of different approaches will possibly lead to even higher orders of multiplexing. Luminescent lanthanide energy transfer probes may be used for a controlled tuning of PL wavelength, intensity, lifetime, and polarization.

4. Ln labels for microscopy

4.1. Application of luminescent Ln labels to luminescence microscopy (LM) and time-resolved luminescence microscopy (TRLM).

As for most luminescent labels, Ln ones have found numerous applications in LM. But interestingly, the history of Ln labels for LM has followed an unconventional way. Basically, the very first Ln labels were very poorly adapted to LM with excitation in the UV domain, the need for UV compatible optical components and rather low brightness of the labels, and all of these drawbacks precluded a friendly use of Ln complexes in LM. Progresses within the field was then essentially guided by the potential benefits associated to a time-gated detection in TRLM.[64] At that time, the main technological difficulty to bypass was the synchronization of the pulsed illumination with the gated detection. The very first setups were implemented with rotating mechanical choppers.[64,115] By varying the width of the slits, the speed of rotation or the phases between excitation and emission choppers,[116] it was possible to control the time of illumination, the delay before acquisition and the duration of acquisition. But such parameters were not easy to handle. The use of pulsed Xe lamps,[64,117] ferro-electric liquid crystals,[116] or acousto-optic modulators[118] further improved the technology, which is nowadays perfectly suited to pulsed LASERs or LEDs triggering a delayed detection obtained by intensified charge coupled device (ICCD) cameras.[64b,119]

At the same time, chemists significantly improved their labels particularly regarding the problems of brightness,[33,45] so that conventional LM became much simpler,[120] with the supplementary advantage of a large Stokes' shift and an improved resistance to photobleaching compared to conventional fluorescent dyes.[30b] Among others, the group of Parker developed numerous Eu based complexes focusing on the relationships between the structures of the compounds and their compartmental localization in cells.[30b,121,122]

Despite these advances, there is still a great deal of interest in TRLM using Ln labels,[123] in particular for the study of FRET processes,[124] as TRLM is one of the rare tools to allow the observation of molecular interactions in the 10 nm range in living organisms. Observation of TR-FRET by TRLM is becoming very popular[125] as an excellent tool to study protein-protein interactions,[126] with the further possibility of colour multiplexing (*vide infra*).

4.2. Multiplexed microscopy

Compared to the many different multiplexed biosensing approaches mentioned in the previous section, multiplexed microscopy with luminescent Ln-probes is a much less developed method. This is most probably caused by the non-standard instrumentation that is required for time-gated Ln PL imaging (*e.g.*, low repetition rate pulsed UV sources, specific microscopy optics adapted to UV excitation light, ICCD cameras) in combination with multicolour detection setups and by the long PL lifetimes. The very long excited-state lifetimes impose excitation at

ARTICLE

low repetition rates (up to a few kHz),which leads to a relatively low photon flux per time compared to conventional fluorophores that have nanosecond excited-state lifetimes (excitation at MHz repetition rate). This low photon flux also makes fluorescence lifetime imaging microscopy (FLIM) a rather complicated or long-acquisition technique for Ln PL. As discussed in the previous section FLIM is not impossible for Ln probes and the development of TR-OSAM[113,114] even permitted multiplexed FLIM that was also shown to be applicable for imaging of labelled *Giardia lamblia* cysts.[114] Apart from the TR-OSAM lifetime multiplexing approach the other two multiplexed microscopy methods use different lanthanide emitters[77,127-134] or FRET from a Ln-donor to different acceptors[135-138] similar to spectroscopy-based multiplexed analysis (cf. multiplexed analysis section). Both the most often used UV-Vis excitable Ln-ions (Tb^{3+}, Eu^{3+}, Dy^{3+}, Sm^{3+})[77,127,128,130-133,135-138] and the standard upconversion excitable Ln-ions (Er^{3+}, Tm^{3+})[73,127,128,134,135] have been applied for multiplexed PL imaging both coordinated in supramolecular complexes[77,127,128,130-133,136-138] or embedded in nanoparticles.[73,127,129,134,135] Although one study reported FRET from UCNPs to dyes for five-colour (Er^{3+} and Tm^{3+} PL and FRET from Er^{3+} to three different dyes) *in-vivo* imaging of UCNPs subcutaneously injected in the back area of nude mice,[135] most of the multiplexed imaging approaches were applied to molecular imaging using *in-vitro* cell cultures. The various multiplexed Ln-based imaging techniques were used for: *(i)* multicolour (incl. FITC) ratiometric imaging of Cu^{2+} (which replaced the Tb^{3+} or Eu^{3+} inside their complexes) in BHK and HeLa cells and folate receptors on HeLa and A549 cells (using folic acid conjugated with Tb^{3+} and Eu^{3+} complexes),[77] *(ii)* duplexed imaging of extracellular biomarkers on fixed MCF-7 cells and fixed tumour tissues using Tb^{3+} and Eu^{3+} complex labelled antibodies,[128,133] *(iii)* duplexed two-photon excitation imaging of fixed T24 cells stained with Tb^{3+} and Eu^{3+} complexes,[130] *(iv)* multiplexed (incl. Pd^{2+} and Pt^{2+} coproporphyrin and Syto 25) imaging of a mixed population of human peripheral blood leukocytes (fixed and permeabilized) using Eu^{3+} and Tb^{3+} complexes labelled to different cell markers,[132] *(v)* ratiometric confocal live cell imaging of pH changes in lysosomes in NIH-3T3 cells using Tb^{3+} and Eu^{3+} complexes,[131] *(vi)* multicolour Tb-to-dye FRET imaging of E- and N-cadherin on fixed MCF-7, A549, and M4-T cells using Tb complex labelled antibodies and various dye-antibody conjugates,[137] *(vii)* extracellular FRET imaging of epidermal growth factor receptor (EGFR) on live A431 cells using Tb^{3+} complex and QD labelled antibodies and intracellular Tb-to-QD FRET and Tb-to-QD-to-dye FRET relays in living HeLa cells using microinjection and cell penetrating peptides,[138] and *(viii)* multiplexed imaging of G-protein coupled receptor (CPCR) oligomerization and internalization using Tb-to-dye and Tb-to-QD FRET.[136]
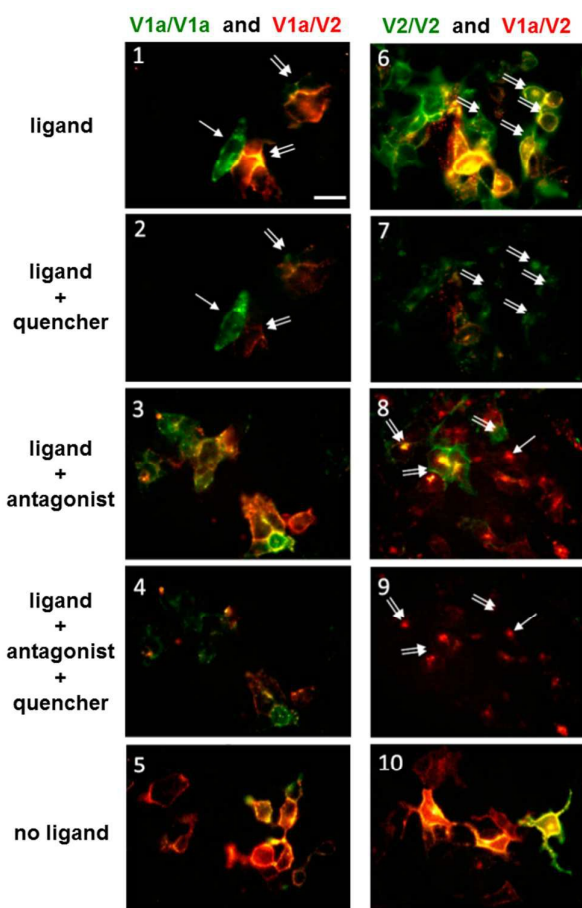

Figure 7. Tb-to-dye FRET imaging of vasopressin V1a and V2 oligomer internalization. Left: HEK 293 cells expressing vasopressin SNAP-V1a and CLIP-V2 receptors are labelled with SNAP-Lumi4-Tb, SNAP-green, and CLIP-red leading to green FRET for V1a oligomers and red FRET for V1a/V2 hetero-oligomers. Right: Labelling of the receptors with CLIP-Lumi4-Tb, CLIP-green, and SNAP-red leads to green FRET for V2 oligomers and red FRET for V1a/V2 hetero-oligomers. Cells were incubated in the presence of vasopressin ligand (25 nM) (1, 2, 6, and 7) or vasopressin ligand (25 nM) and SR121463 antagonist (250 nM) (3, 4, 8, and 9) or without any ligand (5, 10). Images 2, 4, 7, and 9 were acquired after addition of QSY9 (10 nM), a cell surface fluorescence quencher that leads to signal only from cell-internalized fluorophores. Single or double arrows point to cells expressing only one or both receptors, respectively. Scale bar: 25 μm. Reproduced with permission from reference 136. Copyright 2015 FASEB.

For this latter study the authors used HEK 293 cells expressing either vasopressin or dopamine receptors that were fused with different protein fusion tags (SNAP-tag, CLIP-tag, and Halo Tag). The corresponding ligands (which bind to the tags) contained the Tb^{3+} complex Lumi4-Tb, different dyes, or biotin (for the binding of streptavidin conjugated with dyes or QDs) and the different Tb-to-dye FRET images could show homo- or hetero-dimerization of the distinct receptors. As shown in Figure 7 this multicolour time-resolved FRET microscopy (MC-TFM) approach was used to image simultaneously vasopressin V1a and V2 receptor homo- and hetero-oligomers in the same HEK293 cell (Figure 7, images 5 and 10) and to follow internalization of each complex under vasopressin ligand stimulation. Under ligand stimulation (25 nM), V1a/V1a oligomers remained mainly at the cell surface and only internalized in cells that exclusively expressed V1a, whereas V2/V2 oligomers internalized in cells expressing one or both

receptors, and V1a/V2 oligomer internalization remained weak in all cells (Figure7, images 1, 2, 6, 7). Inhibition of V2 receptors with the V2-selective antagonist SR121463 increased V1a oligomer internalization (Figure 7, images 3 and 4), blocked V2 oligomer internalization, and revealed V1/V2 internalization (Figure 7, images 8 and 9).

This example of Ln-based multiplexed imaging shows that the technology is already beyond the proof-of-concept stage and can be used to reveal real biological questions such as the impact of GPCR oligomerization on internalization processes. Taking into account the capabilities that multiplexed biosensing with Ln-ions has already demonstrated in spectroscopic applications (cf. multiplexed analysis section) and the many intra- and extracellular processes and interactions that could be investigated with multiplexed imaging, one can expect much more progresses of multiplexed Ln microscopy in the near future.

4.3. Ln based near infrared luminescence microscopy (NIR-LM).

Water-soluble NIR emitting complexes are very good candidates for optical microscopy and time-resolved fluorescence imaging since their emission matches the 650 nm - 1350 nm spectral window were the light penetration of the tissues is maximum, the scattering of light is low as is the autofluorescence of the samples.[139,140] The PL intensity of NIR-emitting lanthanide complexes is expected to be extremely weak in solution due to highly competitive vibrational quenching of oscillators of the ligand (O-H, N-H and C-H bonds).[25-28] Nevertheless, advances in the instrumentation such as LASER systems and optical amplifiers as well as the improvement of the detector sensitivity have, since the late 90's, prompted the interest for such complexes. One of the first observations of NIR-emission from Ln complexes in solution was achieved with the Tris-(hexafluoroacetylacetonato)Nd^{3+} complex with deuterated hexafluoroacetylacetone ([Nd(HFA-D)]$_3$) in deuterated organic solvents.[141] Characteristic $^4F_{3/2} \rightarrow$ ^4I_J transitions with J = 9/2, 11/2 and 13/2 were observed at 880 nm, 1062 nm and 1345 nm, respectively, with, at best, a PL quantum yield of. 0.6 % in DMSO-d_6 (λ_{ex}= 585 nm).[142] Soon after, typical emission spectra were also recorded in pure water for concentrated Nd^{3+} nitrate and other salts.[143] New antennae have then been developed with the aims *(i)* to improve the sensitization of the Ln^{3+} excited states by shifting the ligand triplet states towards lower energies and *(ii)* to limit vibrational quenching. β-diketonate-based complexes,[144,145] as well as antennae derived from bipyridine,[146] 1,10-phenanthroline,[147] BODIPY,[148] quinoline,[149-151] porphyrin,[152,153] or 2-hydroxyisophtalamide units,[154] have received much attention. The use of *d*-block transition complexes such as Re$^+$, Pt^{2+},[155] Cr^{3+},[156] and Ru^{2+} [157] also led to a wide range of heterobimetallic systems with interesting properties. Several strategies have been developed to limit the presence of high-energy oscillators in

the proximity of the metal center, such as fluorination[158] and deuteration.[159] More particularly, the per-deuteration of bipyridine derivatives gave extremely bright Yb, Nd, Er, Pr[159] as well as Tm complexes.[20,161]

The first Ln^{3+} NIR-emitting bioprobes were developed by Bünzli and coworkers and are based on neutral triple-stranded helicates with ligand L^1 incorporating two Ln^{3+} ions (Figure 8).[162]
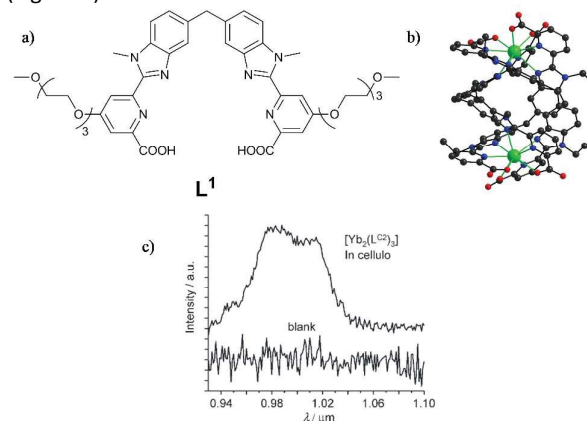
Figure 8: a) Ligand L^1 and b) molecular structure of the [Ln$_2$(L^1)$_3$] helicate (Ln = Tb, H atoms omitted for clarity). c) In cellulo emission spectrum of [Yb$_2$(L^1)$_3$] in HeLa cells.Reproduced with permission from reference 165. Copyright 2008, Wiley-VCH)

Ligand L^1 features two symmetrical tridentate units for the successive binding of two Ln^{3+} ions and Poly(oxyethylene) substituents insure the good water solubility of the system. [163,164] The helicate, Ln$_2$L^1$_3$, displays a high thermodynamic stability in buffered water at physiological pH (log β_{23}^{Ln} = 25(1), Ln = La, Eu, Lu, pH 7.4, Tris-HCl 0.1M, 298K) and is inert towards competition with common chelating agents such as EDTA, citrate and L-ascorbate, although some dissociation is observed in presence of large concentrations of dtpa or Zn^{2+}. Energy transfer to a large variety of Ln^{3+} cations was observed in water, among which Yb^{3+}(ϕ_L^{Yb} = 0.15%, τ_{H2O} = 4.4 μs). The helicates were used to stain HeLa cells. Although NIR-LM was not available at the time, internalization in the cytoplasm was observed with visible analogues (Ln = Sm, Tb, Eu). Moreover, *in cellulo* Yb^{3+} emission spectra were observed (Figure 8c), thus showing for the first time that cell staining with NIR Ln^{3+} emitters was possible, despite their low PL quantum yields.

The first NIR confocal microscopy images with Ln^{3+} probes were obtained 3 years later by the research team of Wong.[165] A water-soluble mitochondria-specific probe was designed from the Yb^{3+} porphyrinate complex YbL^2 (Figure 9). Covalent linkage with Rhodamine B provided water solubility (in the 10 μM concentration range) as well as mitochondria-specific targeting. With a Soret absorption band at *ca.* 430 nm, porphyrin is an appropriate antenna for the population of the $^5F_{5/2}$ energy level of Yb^{3+} and the capping ligand [(η^5-C$_5$H$_5$)Co{(MeO)$_2$P=O}$_3$] was added in order to protect the Yb^{3+} ion from non-radiative deactivations and from solvolysis. As a consequence, very

interesting spectroscopic properties (ϕ_L^{Yb} = 2.5%, τ_{H2O} = 18.1 μs, λ_{exc} = 430 nm) were observed in water.

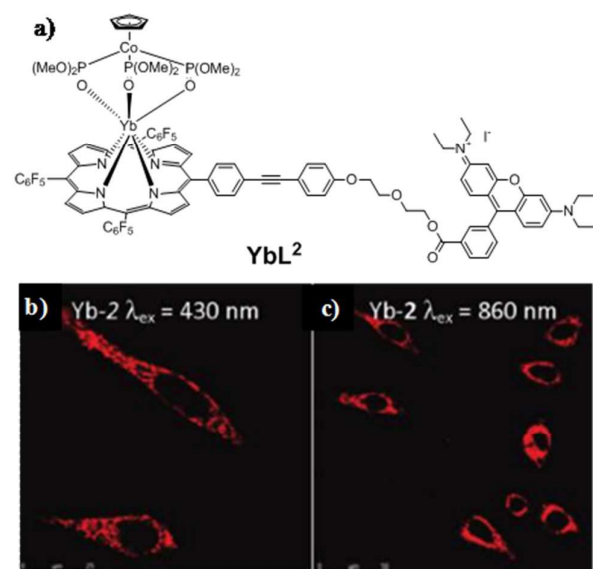**Figure 9:** a) Structure of the YbL^2 complex, b) linear and c) two-photon *in vitro* imaging of HeLa cells (zoom ×40, λ_{em} = 500-800 nm) (reproduced with permission from reference 165. Copyright 2011 American Chemical Society).

Moreover, no significant changes in the NIR emission were observed in the presence of large excess of citrate, bicarbonate, phosphate, HSA, Zn^{2+} and Cu^{2+}, indicating a good stability of the Yb^{3+} complex in these conditions (HEPES, pH 7.4). Negligible influence of the pH was also reported. HeLa cells were incubated with a solution of YbL^2 and classical linear confocal microscopy images (λ_{exc} = 430 nm) showed intense visible emission of the ligand inside the cytoplasm (Figure 9b), with a preferential localization in the mitochondria. An IC_{50} value in the millimolar range was determined, suggesting very minor cytotoxicity. Another significant advantage of such porphyrinate-based probes lies in their nonlinear optical properties, enabling two-photon (σ_2 =375 GM in water, λ_{exc} = 860 nm) and even three-photon excitation (λ_{exc} = 1290 nm). Images were recorded using two-photon confocal NIR-to-visible laser microscopy (Figure 9c), which is a very appealing imaging technique providing non-damageable long wavelength excitation with high spatial confinement and giving images with higher 3D-resolution. Observations were in perfect agreement with linear optical imaging. Such NIR-to-NIR imaging probes with large Stokes shifts are indeed very powerful markers since they are less affected by the scattering of the biological media, thereby enabling the imaging of in-depth tissues.

Proof of concept was achieved by Maury et al. one year later by developing the first NIR-to-NIR confocal laser microscope. They reported a very elegant example of NIR two-photon scanning laser microscopy imaging with two Yb^{3+} complexes, (Yb1 and Yb2, Figure 10).[166]
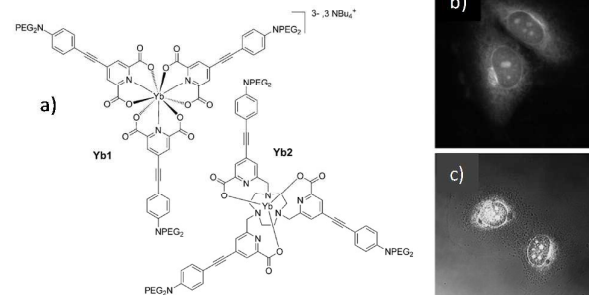

Figure 10. a) Yb complexes, b) linear (λ_{ex} = 450-490 nm, visible emission) and c) two-photon imaging (λ_{ex} = 760 nm, λ_{em} = 491-673 nm) of fixed T24 cells stained with [Yb(L$^-$)$_3$](NBu$_4$)$_3$ (reproduced with permission from reference 166. Copyright 2012, Wiley-VCH).

The two probes are based on (phenyl-ethynyl)-dipicolinic antennae, which are substituted by bis-PEGamino donors in order to obtain push-pull molecules with highly polarizable intra-ligand charge-transfer (ILCT) bands centered at 400 nm[167] and good water solubility. These ILCT bands can be used to populate the $^2F_{5/2}$ excited state of Yb^{3+} by conventional one-photon excitation but, more interestingly, by nonlinear two-photon excitation at 760 nm, as shown by the quadratic dependency of the emission intensity as a function of the incident pump intensity of the LASER. The two-photon absorption cross-section of Yb1 was measured to be 755 GM at 740 nm. The design of the ligand was then improved by incorporating these antennae on a triazacyclononane platform, to yield Yb2, thereby increasing the stability of the complex in water. Similar linear (ϕ_L^{Yb} < 1%, τ_{H2O} = 3 μs, λ_{exc} = 380 nm) and nonlinear optical properties (σ_2 =500 GM in water, λ_{exc} = 380 nm) were reported for the two Yb complexes. In a first place, one- and two-photon scanning microscopy experiments were carried out using conventional microscopes, *i.e.* a wide range epifluorescence setup for one-photon excitation in the visible range and a NIR-to-visible confocal microscope for two-photon excitation. Fixed T24 cancer cells were incubated with Yb1 in PBS-buffered solutions. Both images showed the successful internalization of the complexes and their preferred location on perinuclear areas or nucleoli (Figure 10). A NIR-to-NIR two-photon excitation setup equipped with a Ti-sapphire laser source (λ_{exc} = 760 nm) was then elaborated. NIR-infrared detection was achieved by an avalanche photodiode and residual laser light was removed by addition of a dichroic mirror and interference filters. This setup was used to image brain vasculature of a mouse perfused with Yb2. 100 μm-thick brain slices were successively imaged in order to reconstitute the capillary network. High signal-to-noise ratio was achieved down to 80 μm depths and this pioneering work clearly demonstrated the potential of NIR-to-NIR two-photon excitation with Ln^{3+} bioprobes for imaging of strongly scattering thick tissues.

The work of Petoud and his collaborators has been focused on providing new nano-objects with a high density

of Ln^{3+} probes in order to significantly increase the signal-to-noise ratio of NIR images. The first study was focused on the synthesis of nanoscale metal-organic frameworks (MOFs) with Yb^{3+} ions and phenylenevinylenedicarboxylate (PVDC) antennae (Figure 11).[168] PVDC was chosen because it displays two intense absorption bands centered at 340 nm and 415 nm, which can be used to populate the $^2F_{5/2}$ excited state of Yb^{3+} by "antenna effect" (Figure 11).
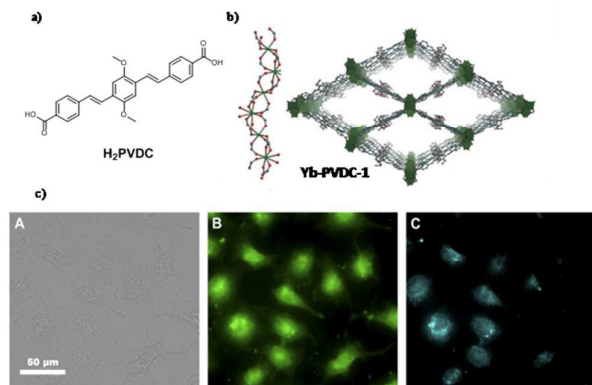

Figure 11.a) PVDC antenna, b) crystal structures of the of the MOFs and c) isible and NIR confocal microscopy imaging of HeLa cells incubated with nano-Yb-PVDC-3 MOFs (λ_{ex} = 377 nm) : (A) Bright-field, (B) λ_{em} = 445 nm, (C) λ_{em} = 770 nm (reproduced with permission from reference 168).

Exciting in PVDC gives rise to typical Yb^{3+} emission(ϕ_L^{Yb} = 0.01%, τ_{H2O} = 7.0 μs, λ_{exc} = 450 nm). Internalization of the nano-MOFs in human HeLa cells and mouse NIH 3T3 cells, together with preferential localization in the cytoplasm, were observed by confocal microscopy experiments (λ_{exc} = 365 nm, λ_{em} = 445 nm) and NIR epifluorescence microscopy on living cells (Figure 11). Moreover, the nano-MOFs show relatively low toxicity (IC$_{50}$ = 50 μg/mL).

A second approach was focused on the use of polyamidoamine dendrimers with 2,3-naphthalamide chromophores and Sm emitters.[169] Sm possesses the dual advantage to be observable by visible confocal and epifluorescence microscopy, due to the emission of the $^4G_{5/2} \rightarrow {}^6H_J$ transitions (J = 5/2, 7/2, 9/2, 11/2) in the 500 - 750 nm range, and also by NIR epifluorescence microscopy because of the $^4G_{5/2} \rightarrow {}^6F_J$ transitions (J = 1/2, 3/2, 5/2, 7/2, 9/2) in the 800 - 1200 nm range. G3P dendrimers substituted by thirty-two 2,3-naphthalamide units were synthesized and complexes with eight equivalents of Sm(NO$_3$)$_3$, leading to spherical species with a hydrodynamic diameter of 8 nm. Typical absorption bands of the 2,3-naphthalamide were observed at 290, 342 and 359 nm, from which energy transfer to the Sm^{3+} $^4G_{5/2}$ excited state (at 20280 cm^{-1}) was observed, hence leading to typical Sm^{3+} emission ($\phi_L^{Yb}({}^4G_{5/2}\rightarrow{}^6H_J)$ = 0.02% and $\phi_L^{Yb}({}^4G_{5/2}\rightarrow{}^6F_J)$ = 8.10^{-4}%,τ_{DMSO} = 15.1 μs, λ_{exc} = 320-340 nm in DMSO). Microscopy experiments on living HeLa cells incubated with Sm dendrimers confirmed its intracellular uptake and showed preferential accumulation in the cytoplasm.

Another approach classically used to increase the local concentration of tracers is to attach them to a surface of a nanoparticle. A recent example was reported by Huang et

al., who linked visible and NIR-emitting complexes to mesoporous silica nanospheres.[170] Ternary β-diketonate complexes with 2-theonyltrifluoroacetonate and 2-(thiophen)imidazo[4,5-*f*][1,10]phenanthroline antennae were chosen since they can either provide visible emission (with Ln = Eu, Sm) or NIR emission (with Ln = Sm, Nd, Yb) upon excitation in the visible (λ_{exc} = 300-405 nm).[171] These complexes were covalently linked to mesoporous silica nanospheres, providing a homogeneous distribution of the complexes around the nanoparticle and preventing their leaching out of the matrix. As a proof of concept, cytotoxicity (IC$_{50}$> 800 μg.mL^{-1}) and cell distribution were measured on living HeLa cells after incubation with Eu-functionalized nanoparticles, and laser scanning luminescence microscopy images showed preferential localization in the cytosol. Unfortunately, neither quantitative information about NIR-emitting nanospheres, nor NIR-images were provided and this was probably due to the lack of accessibility to a NIR-imaging setup.

In order to remove this experimental barrier and to promote the development of NIR-imaging, a very interesting experimental setup was recently proposed to monitor NIR emission by using a piezo scanning confocal fluorescence microscope initially working in the visible range only.[172] The standard UV/Vis CCD camera was replaced by a silicon-based CCD detector working in the NIR and one additional long-path filter was added to separate excitation light from emission. This new device is very powerful since it enables the monitoring of the emission spectrum of each pixel. Its efficiency was first demonstrated by imaging lanthanide complexes (Ln = Eu, Nd, Yb) with phenacyl-DO3A derivatives. The phenacyl chromophore enables the sensitization of Eu, Nd, Yb upon the visible excitation (λ_{ex} = 405 nm) provided by a conventional microscopy setups. Typical emission spectra as well as spectrally resolved images could be recorded in D$_2$O solutions (in the 0.1 − 1 mM concentration range) and also on powder samples of silica nanoparticles impregnated with the complexes. Silica beads labeled with a Nd complex could be observed as well as characteristic Nd emission around 875 nm corresponding to the $^4F_{3/2} \rightarrow {}^4I_{9/2}$ transition.

In conclusion, it is clear that luminescent reporters based on NIR-emitting lanthanide complexes (Er, Nd, Yb, Sm and Ho) are strong candidates for imaging, and in particular for the imaging of thick tissues showing strong scattering. However, their success has been so far hindered by the lack of adequate instrumentation and by their low quantum yields in water. NIR-epifluorescence imaging systems are commercially available and several home-built setups have now been assembled in order to perform spectrally resolved one-photon visible-to-NIR and two-photon NIR-to-NIR optical microscopy. Moreover, several strategies are under investigation in order to boost the brightness of the tracers, leading to great improvement in their sensitivity.

ChemComm

ARTICLE

5. Perspectives for Ln-based biolabelling.

In addition to the improvements originating from the spectroscopic properties of Ln biolabels mentioned in the previous sections, interesting perspectives in the field could be gained by the use of polymetallic Ln biolabels and their applications to multimodal imaging. In the case of dual optical/magnetic resonance imaging, the topic has recently been covered by different authors.[173,174] For association with positron emission tomography (PET), Ln nanoparticles were also demonstrated to be efficient phosphors upon excitation by X-rays or 18F radioisotope.[175] Eu salts have also been shown to be luminescent upon excitation by Cerenkov photons originating from desintegration of ^{18}F or [74]As.[176]

Finally, although the topic is still in its infancy, it is believed that molecular based Ln upconverting (UC) labels may become a target of choice for biolabeling. Similar to UCNPs these probes would be particularly well suited for low background analytical and imaging applications while offering the advantage of molecular sizes. Since the very first proof of concept provided by Piguet and coworkers in 2011,[177,178] on an heterotrinuclear triple helicate of Cr and Er showing UC in organic solutions up to 150 K, the topic has gradually evolved with observation of UC in Tm complexes in DMSO at r.t.[179] as well as for an Er complex in CDCl$_3$ solution also at r.t.[180] One of the last steps before application to aqueous media was the observation of UC in D$_2$O in an Er dimer[181] issued from some works on supramolecular Ln assemblies.[182] If these systems are still rather inefficient regarding photon UC in solution, there is significant space for large improvements and possible applications to bioanalysis.

6. Conclusions

Luminescent Ln complexes and their applications to biolabelling and bioanalytical applications are still some flourishing topics and, undoubtedly, their future will see the emergence of new structures, new ideas and new applications allowing for the development of ever more sensitive and efficient bioanalytical sensors. We sincerely hope that this feature article will transmit our enthusiasm for these research topics to the younger generation, as it was the case for us some few years ago,[13b] and we are sure that Ln-based biolabelling will continue to populate our long-lived excitation and motivation.

References

1   R.S. Yalow, and S.A. Berson, *J. Clin. Invest.* **1960**, *39*, 1157.
2   A. Mayer, and S. Neuenhofer, *Angew. Chem. Int. Ed.* **1994**, *33*, 1044.
3   L.D. Lavis, and R.T. Raines *ACS Chem. Biol.* **2008**, *3*, 142.
4   H.V. Ai, *Anal. Bioanal. Chem.* **2015**, *407*, 9.
5   I.L. Medintz, H. T. Uyeda, E.R. Goldman, and H. Mattoussi, *Nature Mat.* **2005**, *4*, 435.
6   J.-C.G. Bünzli, and C. Piguet, *Chem. Soc. Rev.* **2005**, *34*, 1048.
7   M.C. Heffern, L.M. Matosziuk, and T. Meade, *Chem. Rev.* **2014**, *114*, 4496.
8   A.K. Hagan, and T. Zuchner, *Anal. Bioanal. Chem.* **2011**, *400*, 2847.
9   W. Zheng, P. Huang, D. Tu, E. Ma, H. Zhu, and X. Chen, *Chem. Soc. Rev.* **2015**, *44*, 1379.
10 W. Zheng, D. Tu, P. Huang, S. Zhou, Z. Chenb, and X. Chen *Chem. Commun.* **2015**, *51*, 4129.
11 K. Binnemans, *Chem. Rev.* **2009**, *109*, 4283.
12 S.T. Frey, and W.D.W. Horrocks *Inorg. Chim. Acta*, **1995**, *229*, 383.
13 a) J.C.G. Bünzli *Coord. Chem. Rev.* **2015**, *293-294*, 19. b) D. Parker, R.S. Dickins, H. Puschmann, C. Crossland, and J.A.K. Howard, *Chem. Soc. Rev.* **2002**, *102*, 1977.
14 S.I. Weissman *J. Chem. Phys.* **1942**, *10*, 214.
15 B. Alpha, R. Ballardini, V. Balzani, J.-M. Lehn, S. Perathoner, and N. Sabbatini *Photochem. Photobiol.* **1990**, *52*, 299.
16 S. Quici, M. Cavazzini, G. Marzanni, G. Accorsi, N. Armaroli, B. Ventura, and F. Barigelletti, *Inorg. Chem.*, **2005**, *44*, 529.
17 J. Zhang, and S. Petoud, *Chem. Eur. J.* **2008**, *14*, 1264.
18 M. Latvaa, H. Takalo, V.-M. Mukkala, C. Matachescu, J. C. Rodriguez-Ubis, and J. Kankare, *J. Lumin.* **1997**, *75*, 149.
19 F.J. Steemers, W. Verboom, D.N. Reinhoudt, E.B. van der Tal, and J.W. Verhoeven, *J. Am. Chem. Soc.* **1995**, *117*, 9408.
20 C. Doffek, and M. Seitz, *Angew. Chem. Int. Ed.* **2015**, *54*, 9719.
21 I. Hemmilä, *J. Alloys Cpds* **1995**, *225*, 480.
22 N. Weibel, L.J. Charbonnière, M. Guardigli, A. Roda, and R. Ziessel *J. Am. Chem. Soc.* **2004**, *126*, 4888.
23 W.deW. Horrocks Jr, and D.R. Sudnick, *J. Am. Chem. Soc.* **1979**, *101*, 334.
24 A. Beeby, I.M. Clarkson, R.S. Dickins, S. Faulkner, D. Parker, L. Royle, A.S.de Sousa, J.A.G. Williams, and M. Woods, *J. Chem. Soc., Perkin Trans.* 2, **1999**, 493.
25 R.M. Supkowski, and W.D. Horrocks Jr., *Inorg. Chim. Acta* **2002**, *340*, 44.
26 T. Kimura, and Y. Kato, *J. Alloys Compd.* **1998**, *275-277*, 806.
27 A. Beeby, B.P. Burton-Pye, S. Faulkner, G.R. Motson, J.C. Jeffery, J.A. McCleverty, and M.D. Ward, *J. Chem. Soc. Dalton Trans.* **2002**, 1923.
28 C. Bischof, J. Wahsner, J. Scholten, S. Trosien, and M. Seitz, *J. Am. Chem. Soc.* **2010**, *132*, 14334.
29 G. Nocton, A. Nonat, C. Gateau, and M. Mazzanti, *Helv. Chim. Acta*, **2009**, *92*, 2257.
30 a) J.W. Walton, A. Bourdolle, S.J. Butler, M. Soulie, M. Delbianco, B.K. McMahon, R. Pal, H. Puschmann, J.M. Zwier, L. Lamarque, O. Maury, C. Andraud, and D. Parker, *Chem. Commun.* **2013**, *49*, 1600. b) S.J. Butler, L. Lamarque, R. Pal, and David Parker, *Chem. Sci.* **2014**, *5*, 1570.
31 I. Lukes, J. Kotek, P. Vojtisek, and P. Hermann, *Coord. Chem. Rev.* **2001**, *216-217*, 287.

ChemComm Accepted Manuscript

32 B. Alpha, J.-M. Lehn, G. Mathis, G. *Angew. Chem. Int. Ed.***1987**, *26*, 266.

33 J. Xu, T.M. Corneillie, E.G. Moore, G.-L. Law, N.G. Butlin, K.N. Raymond, *J. Am. Chem. Soc.*, **2011**, *133*, 19900.

34 A.D. Sherry, J. Ren, J. Huskens, E. Brücher, E. Toth, C.F.C.G. Geraldes, M.M.C.A. Castro, and W.P. Cacheris, *Inorg. Chem.* **1996**, *35*, 4604.

35 a) M. Elhabiri, S. Abada, M. Sy, A. Nonat, P. Choquet, D. Esteban-Gomez, C. Cassino, C. Platas-Iglesias, M. Botta, and L.J. Charbonnière, *Chem. Eur. J.* **2015**, *21*, 6535. b) S. Abada, A. Lecointre, M. Elhabiri, D. Esteban-Gomez, C. Platas-Iglesias, G. Tallec, M. Mazzanti, and L.J. Charbonnière, *Chem. Commun.* **2012**, *48*, 4085.

36 M. Elhabiri, R. Scopelitti, J.-C.G. Bünzli, and C. Piguet, *J. Am. Chem. Soc.* **1999**, *121*, 10747.

37 H. Bazin, M. Préaudat, E. Trinquet, and G. Mathis *Spectrochimica Acta A*, **2001**, *57*, 2197.

38 J.L. Toner, US patent 4 837 169.

39 A. K. Saha, K. Kross, E.D. Kloszewski, D.A. Upson, J.L. Toner, R.A. Snow, C. D. V. Black, and V. C. Desai *J. Am. Chem. Soc.* **1993**, *115*, 11032.

40 P.A. Tanner, *Chem. Soc. Rev.* **2013**, *42*, 5090.

41 N. Weibel, L.J. Charbonnière, M. Guardigli, A. Roda, and R. Ziessel *J. Am. Chem. Soc.* **2004**, *126*, 4888.

42 a) N. Hildebrandt, L.J. Charbonnière, M. Beck, R.F. Ziessel, and H.G. Löhmannsröben, *Angew. Chem. Int. Ed.* **2005**, *44*, 7612. b) N. Hildebrandt, L.J. Charbonnière, and H.-G. Löhmannsröben, *J. Biomed. Biotech.* **2007**, 79169.

43 A. D'Aléo, A. Picot, P.L. Baldeck, C. Andraud, and O. Maury, *Inorg. Chem.* **2008**, *47*, 10269.

44 M. Delbianco, L. Lamarque and D. Parker, *Org. Biomol. Chem.* **2014**, *12*, 8061.

45 S.J. Butler, M. Delbianco, N.H. Evans, A.T. Frawley, R. Pal, D. Parker, R.S. Puckrin, and D.S. Yufit, *Dalton Trans.* **2014**, *43*, 5721.

46 see for examples : a) J. Yuan, G. Wang, K. Majima, and K. Matsumoto, *Anal. Chem.* **2001**, *73*, 1869. b) C. Song, Z. Ye, G. Wang, J. Yuan, and Y. Guan, *ACS Nano* **2010**, *4*, 5389. c) A.S. Chauvin, S. Comby, B. Song, C.D.B. Vandevyver, and J.-C.G. Bünzli, *Chem. Eur. J.* **2008**, *14*, 1726.

47 a) S. Poupart, C. Boudou, P. Peixoto, M. Massonneau, P.-Y. Renard, and A. Romieu, *Org. Biomol. Chem.*, **2006**, *4*, 4165.b) M.K. Johansson, R.M. Cook, J. Xu, and K.N. Raymond, *J. Am. Chem. Soc.* **2004**, *126*, 16451.

48 J. Hovinen, *Chem. Biodivers.* **2006**, *3*, 296.

49 H. Takalo, V.-M. Mukkala, H. Mikola, P. Liitti, and I. Hemmila, *Bioconj. Chem.* **1994**, *5*, 278.

50 a) K. Mitrunen, K. Pettersson, T. Piironen, T. Bjork, H. Lilja, and T. Lövgren, *Clin. Chem.* **1995**, *41*, 1115. b) H. Takalo, I. Hemmilä, T. Sutela, and M. Latva, *Helv. Chim. Acta.*, **1996**, *79*, 789.

51 H. Takalo, E. Hänninen, and J. Kankare, *Helv. Chim. Acta.* **1993**, *76*, 877.

52 R.A. Evangelista, A. Pollak, B. Allore, E.F. Templeton, R.C. Morton, and E.P. Diamandis, *Clin. Biochem.* **1988**, *21*, 173.

53 a) K. Sasamoto, D. Horiguchi, M. Nobuhara, and H. Mochizuki, Japan Patent 405268/90, 08/07/1992. b) J. Yuan, and K. Matsumoto, K. *Anal. Chem.* **1998**, *70*, 596-601.

54 a) V.M. Mukkala, M. Helenius, I. Hemmilä, J. Kankare, and H. Takalo, *Helv. Chim. Acta* **1993**, *76*, 1361. b) V.M. Mukala, H. Takalo, P. Liitti, and I. Hemmilä, *J. Alloys Comp.* **1995**, *225*, 507.

55 P. de Hoog, P. Gamez, W.L. Driessen, and J. Reedijk, *Tetrahedron Lett.* **2002**, *43*, 6783.

56 S. Claudel-Gillet, J. Steibel, N. Weibel, T. Chauvin, M. Port, I. Raynal, E. Toth, R.F. Ziessel, and Charbonnière *Eur. J. Inorg. Chem.* **2008**, 2856.

57 M. Starck, P. Kadjane, E. Bois, B. Darbouret, A. Incamps, R. Ziessel, and L.J. Charbonnière *Chem. Eur. J.* **2011**, *17*, 9164.

58 K. Nchimi-Nono, K.D. Wegner, S. Lindén, A. Lecointre, L. Ehret-Sabatier, S. Shakir, N. Hildebrandt, and L.J. Charbonnière *Org. Biomol. Chem.* **2013**, *11*, 6493.

59 A. Beck, E. Wagner-Rousset, D. Ayoub, A. Van Dorsselaer, and S. Sanglier-Cianférani, *Anal. Chem.* **2013**, *85*, 715.

60 J. Hovinen, *Bioconjugate Chem.* **2007**, *18*, 597.

61 P. Ge, and P.R. Selvin, *Bioconjugate Chem.* **2003**, *14*, 870.

62 see for example a) M. Kwiatkowski, M. Samiotaki, U. Lamminmäki, V.-M. Mukkala, and U. Landegren, *Nucl. Acids Res.* **1994**, *22*, 2604. b)H. Hakala, P. Ollikka, J. Degerholm, and J. Hovinen, *Tetrahedron* **2002**, *58*, 8771. c) J. Hovinen, and H. Hakala, *Org. Lett.* **2001**, *3*, 2473. d) L. Jaakkola, J. Peuralahti, H. Hakala, J. Kunttu, P. Tallqvist, V.M. Mukkala, A. Ylikoski, and J. Hovinen, *Bioconjugate Chem.* **2005**, *16*, 700.

63 I. Hemmila, and V.M. Mukkala, *Crit. Rev. Clin. Lab. Sci.* **2001**, *38*, 441.

64 a) N.P. Verwoerd, E.J. Hennink, J. Bonnet, C.R.G. Van der Geest, and H.J. Tanke *Cytometry*, **1994**, *16*, 113. b) L.J. Charbonnière, R. Ziessel, M. Guardigli, A. Roda, N. Sabbatini, and M. Cesario *J. Am. Chem. Soc.* **2001**, *123*, 2436.

65 I. Hemmilä, and R. Harju, in *Bioanalytical applications of labelling technologies*, I. Hemmilä, T. Stählberg, and P. Mottram Eds, Wallac Oy and EG&G Cie Pb., 1995, Turku, Finland, Chap. 5, p. 83.

66 J.M. Zwier, H. Bazin, L. Lamarque, and G. Mathis *Inorg. Chem.* **2014**, *53*, 1854.

67 a) B. Valeur in *Molecular Fluorescence: Principles and Applications*, Wiley-VCH, Weinheim, 2002. b) L.J. Charbonnière, and N. Hildebrandt *Eur. J. Inorg. Chem.* **2008**, 3241.

68 M. Elbanowski, and B. Makowska, *J. Photochem. Photobiol. A, Chem.* **1996**, *99*, 85.

69 V. Hagren P. von Lode, A. Syrjälä, T. Soukka, T. Lövgren, H. Kojola, and J. Nurmi *Anal Biochem.* **2008**, *374*, 411.

70 H. Chen, Y. Lang, Y. Zhang, D. Zhao, G. Qin, C. Wu, K. Zheng and W. Qin, *J. Mat. Chem. C*, **2015**, *3*, 6314.

71 Y. Chen and Y. Zhang, *Nanosci. Nanotech. Letters*, **2013**, *5*, 237.

72 R. E. Gerver, R. Gomez-Sjoeberg, B. C. Baxter, K. S. Thorn, P. M. Fordyce, C. A. Diaz-Botia, B. A. Helms and J. L. DeRisi, *Lab on a Chip*, **2012**, *12*, 4716.

73 H. H. Gorris and O. S. Wolfbeis, *Ang. Chem. Int. Ed.*, **2013**, *52*, 3584.

74 H. Härmä, G. Sarrail, J. Kirjavainen, E. Martikkala, I. Hemmilä and P. Hänninen, *Anal. Chem.*, **2010**, *82*, 892.

75 Y. Huang, H. Zhang, X. Chen, X. Wang, N. Duan, S. Wu, B. Xu and Z. Wang, *Biosens. Bioelectron.*, **2015**, *74*, 170.

76 Y. A. Li, S. K. Ren, Q. K. Liu, J. P. Ma, X. Y. Chen, H. M. Zhu and Y. B. Dong, *Inorg. Chem.*, **2012**, *51*, 9629.

77 J. Liu, J. Liu, W. Liu, H. Zhang, Z. Yang, B. Wang, F. Chen and H. Chen, *Inorg. Chem.*, **2015**, *54*, 7725.

78 K. Murray, Y.-C. Cao, S. Ali and Q. Hanley, *Analyst*, **2010**, *135*, 2132.

79 E. Pershagen and K. E. Borbas, *Ang. Chem. Int. Ed.*, **2015**, *54*, 1787.

80 F. Wang and X. Liu, *Acc. Chem. Res.*, **2014**, *47*, 1378.

81 L. Wang, H. Chen, D. Zhang, D. Zhao and W. Qin, *Mater. Lett.*, **2011**, *65*, 504.

82 Y. Zhang, L. Zhang, R. Deng, J. Tian, Y. Zong, D. Jin and X. Liu, *J. Amer. Chem. Soc.*, **2014**, *136*, 4893.

83 F. Wang, X. P. Fan, M. Q. Wang and Y. Zhang, *Nanotechn.*, **2007**, *18*, 025701.

84 F. Wang and X. G. Liu, *J. Am. Chem. Soc.*, **2008**, *130*, 5642.

85 F. Wang, X. J. Xue and X. G. Liu, *Ang. Chem. Int. Ed.*, **2008**, *47*, 906.

86 E. Pershagen and K. E. Borbas, *Coord. Chem. Rev.*, **2014**, *273*, 30.

87 E. Pershagen, J. Nordholm and K. E. Borbas, *J. Am. Chem. Soc.*, **2012**, *134*, 9832.

88 W. R. Algar, A. P. Malanoski, K. Susumu, M. H. Stewart, N. Hildebrandt and I. L. Medintz, *Anal. Chem.*, **2012**, *84*, 10136.

89 W. R. Algar, D. Wegner, A. L. Huston, J. B. Blanco-Canosa, M. H. Stewart, A. Armstrong, P. E. Dawson, N. Hildebrandt and I. L. Medintz, *J. Am. Chem. Soc.*, **2012**, *134*, 1876.

90 J. C. Claussen, W. R. Algar, N. Hildebrandt, K. Susumu, M. G. Ancona and I. L. Medintz, *Nanoscale*, **2013**, *5*, 12156.

91 J. C. Claussen, N. Hildebrandt, K. Susumu, M. G. Ancona and I. L. Medintz, *ACS Appl. Mater. Interfaces*, **2014**, *6*, 3771.

92 D. Geißler, L. J. Charbonnière, R. F. Ziessel, N. G. Butlin, H. G. Löhmannsroben and N. Hildebrandt, *Ang. Chem. Int. Ed.*, **2010**, *49*, 1396.

93 D. Geißler, S. Linden, K. Liermann, K. D. Wegner, L. J. Charbonnière and N. Hildebrandt, *Inorg. Chem.*, **2014**, *53*, 1824.

94 T. Hilal, V. Puetter, C. Otto, K. Parczyk and B. Bader, *J. Biomol. Screen*, **2010**, *15*, 268.

95 N. Hildebrandt, K. D. Wegner and W. R. Algar, *Coord. Chem. Rev.*, **2014**, *273*, 125.

96 M. Jeyakumar and J. A. Katzenellenbogen, *Anal. Biochem.*, **2009**, *386*, 73.

97 Z. W. Jin, D. Geißler, X. Qiu, K. D. Wegner and N. Hildebrandt, *Ang. Chem. Int. Ed.*, **2015**, *54*, 10024.

98 S. H. Kim, J. R. Gunther and J. A. Katzenellenbogen, *J. Am. Chem. Soc.*, **2010**, *132*, 4685.

99 T. Kokko, L. Kokko and T. Soukka, *J. Fluoresc.*, **2009**, *19*, 159.

100 T. Kokko, T. Liljenback, M. T. Peltola, L. Kokko and T. Soukka, *Anal. Chem.*, **2008**, *80*, 9763.

101 K. R. Kupcho, D. K. Stafslien, T. DeRosier, T. M. Hallis, M. S. Ozers and K. W. Vogel, *J. Am. Chem. Soc.*, **2007**, *129*, 13372.

102 A. M. Lipchik, M. Perez, W. Cui and L. L. Parker, *Anal. Chem.*, **2015**, *87*, 7555.

103 F. Morgner, D. Geissler, S. Stufler, N. G. Butlin, H.-G. Loehmannsroeben and N. Hildebrandt, *Ang. Chem. Int. Ed.*, **2010**, *49*, 7570.

104 X. Qiu and N. Hildebrandt, *ACS Nano.*, **2015**, *9*, 8449.

105 T. Rantanen, M.-L. Jarvenpaa, J. Vuojola, R. Arppe, K. Kuningas and T. Soukka, *Analyst*, **2009**, *134*, 1713.

106 K.D. Wegner, Z.W. Jin, S. Linden, T.L. Jennings, and N. Hildebrandt, *ACS Nano* **2013**, *7*, 7411.

107 K. D. Wegner, P. T. Lanh, T. Jennings, E. Oh, V. Jain, S. M. Fairclough, J. M. Smith, E. Giovanelli, N. Lequeux, T. Pons and N. Hildebrandt, *ACS Appl. Mater. Interfaces*, **2013**, *5*, 2881.

108 K. D. Wegner, S. Linden, Z. W. Jin, T. L. Jennings, R. el Khoulati, P. M. P. van Bergen en Henegouwen and N. Hildebrandt, *Small*, **2014**, *10*, 734.

109 K. D. Wegner, F. Morgner, E. Oh, R. Goswami, K. Susumu, M. H. Stewart, I. L. Medintz and N. Hildebrandt, *Chem. Mater.*, **2014**, *26*, 4299.

110 D. Geißler, S. Stufler, H. G. Löhmannsroben and N. Hildebrandt, *J. Am. Chem. Soc.*, **2013**, *135*, 1102.

111 M. Massey, M. G. Ancona, I. L. Medintz and W. R. Algar, *ACS Photonics*, **2015**, *2*, 639.

112 M. Massey, M. G. Ancona, I. L. Medintz and W. R. Algar, *Anal. Chem.*, **2015**, *87*, 11923.

113 Y. Q. Lu, J. Lu, J. B. Zhao, J. Cusido, F. M. Raymo, J. L. Yuan, S. Yang, R. C. Leif, Y. J. Huo, J. A. Piper, J. P.

Robinson, E. M. Goldys and D. Y. Jin, *Nat. Commun.*, **2014**, *5*, 3741.

114 Y. Q. Lu, J. B. Zhao, R. Zhang, Y. J. Liu, D. M. Liu, E. M. Goldys, X. S. Yang, P. Xi, A. Sunna, J. Lu, Y. Shi, R. C. Leif, Y. J. Huo, J. Shen, J. A. Piper, J. P. Robinson and D. Y. Jin, *Nat. Photonics*, **2014**, *8*, 33.

115 T.M. Jovin, D.J. Arndt-Jovin *Annu. Rev. Biochem. Biophys. Chem.* **1989**, *18*, 271.

116 G. Marriott, R.M. Clegg, D.J. Arndt-Jovin, and T.M. Jovin, *Biophys. J.* **1991**, *60*, 1374.

117 L. Seveus, M. Väisälä, S. Syrjänen, M. Sandberg, A. Kuuisto, R. Harju, J. Salo, I. Hemmilä, H. Kojola, E. Soini, *Cytometry*, **1992**, *13*, 329.

118 E J. Hennink, R. de Haas, N.P. Verwoerd, and H J. Tanke *Cytometry*, **1996**, *24*, 312.

119 a) S. Ghose, E. Trinquet, M. Laget, H. Bazin, and G. Mathis *J. Alloys Cpds* **2008**, *451*, 35. b) L.J. Charbonnière, N. Weibel, C. Estournes, C. Leuvrey, R. Ziessel *New J. Chem.* **2004**, *28*, 777.

120 see for example : a) V. Divya, V. Sankar, K. G. Raghub, and M. L. P. Reddy *Dalton Trans.* **2013**, *42*, 12317. b) R. Pal, D. Parker, *Org. Biomol. Chem.* **2008**, *6*, 1020. c) A.S. Chauvin, S. Comby, B. Song, C.D.B. Vandevyver, and J.-C.G. Bünzli, *Chem. Eur. J.* **2008**, *14*, 1726. d) D.J. Bornhop, D.S. Hubbard, M.P. Houlne, C. Adair, G.E. Kiefer, B.C. Pence, and D.L. Morgan, *Anal. Chem.* **1999**, *71*, 2607.

121 E.J. New, D. Parker, D.G. Smith, and J.W. Walton, *Cur. Op. Chem. Biol.* **2010**, *14*, 238.

122 M. Starck, R. Pal, and D. Parker, *Chem. Eur. J.* **2016**, *22*, 570.

123 B. Song, C.D.B. Vandevyver, A.-S. Chauvin, and J.-C.G. Bünzli, *Org. Biomol. Chem.* **2008**, *6*, 4125.

124 M. Delbianco, V. Sadovnikova, E. Bourrier, G. Mathis, L. Lamarque, J.M. Zwier, and D. Parker, *Angew. Chem. Int. Ed.* **2014**, *53*, 10718.

125 M. Rajendran, and L.W. Miller *Biophys. J.* **2015**, *109*, 240.

126 H.E. Rajapakse, N. Gahlaut, S Mohandessi, D. Yu, J.R. Turner, and L.W. Miller *Proc. Nat. Acad. Sci.* **2010**, *107*, 13582.

127 J. C. G. Bünzli, *Chem. Rev.*, **2010**, *110*, 2729.

128 V. Fernandez-Moreira, B. Song, V. Sivagnanam, A. S. Chauvin, C. D. B. Vandevyver, M. Gijs, I. Hemmilä, H. A. Lehr and J. C. G. Bünzli, *Analyst*, **2010**, *135*, 42.

129 Y. I. Park, K. T. Lee, Y. D. Suh and T. Hyeon, *Chem. Soc. Rev.*, **2015**, *44*, 1302.

130 V. Placide, A. T. Bui, A. Grichine, A. Duperray, D. Pitrat, C. Andraud and O. Maury, *Dalton Transactions*, **2015**, *44*, 4918.

131 D. G. Smith, B. K. McMahon, R. Pal and D. Parker, *Chem. Commun.*, **2012**, *48*, 8520.

132 A. E. Soini, A. Kuusisto, N. J. Meltola, E. Soini and L. Seveus, *Microsc. Res. Tech.*, **2003**, *62*, 396.

133 B. Song, V. Sivagnanam, C. D. B. Vandevyver, I. Hemmilä, H.-A. Lehr, M. A. M. Gijs and J.-C. G. Bünzli, *Analyst*, **2009**, *134*, 1991.

134 F. Wang, R. Deng, J. Wang, Q. Wang, Y. Han, H. Zhu, X. Chen and X. Liu, *Nature Mater.*, **2011**, *10*, 968.

135 L. Cheng, K. Yang, M. Shao, S.-T. Lee and Z. Liu, *J. Phys. Chem. C*, **2011**, *115*, 2686.

136 O. Faklaris, M. Cottet, A. Falco, B. Villier, M. Laget, J. M. Zwier, E. Trinquet, B. Mouillac, J. P. Pin and T. Durroux, *FASEB J.*, **2015**, *29*, 2235.

137 S. Linden, M. K. Singh, K. D. Wegner, M. Regairaz, F. Dautry, F. Treussart and N. Hildebrandt, *Dalton Trans.*, **2015**, *44*, 4994.

138 H. Samareh Afsari, M. Cardoso Dos Santos, S. Lindén, T. Chen, X. Qiu, P. M. P. van Bergen en Henegouwen, T. L.

Jennings, K. Susumu, I. L. Medintz, N. Hildebrandt and L. W. Miller, *submitted*, 2015.

139 A. M. Smith, M. C. Mancini and S. Nie, *Nat. Nanotechnol.*, **2009**, *4*, 710.

140 L. Yuan, W. Lin, K. Zheng, L. He, and W. Huang, *Chem. Soc. Rev.* **2013**, *42*, 622.

141 Y. Hasegawa, K. Murakoshi, Y. Wada, S. Yanagida, J.-H. Kim, N. Nakashima and T. Yamanaka, *Chem. Phys. Lett.*, 1996, **248**, 8.

142 Y. Hasegawa, Y. Kimura, K. Murakoshi, Y. Wada, J.-H. Kim, N. Nakashima, T. Yamanaka and S. Yanagida, *J. Phys. Chem.*, 1996, **100**, 10201.

143 A. Beeby and S. Faulkner, *Chem. Phys. Lett.*, 1997, **266**, 116.

144 N. M. Shavaleev, S. J. A. Pope, Z. R. Bell, S. Faulkner and M. D. Ward, *Dalton Trans*, 2003, 808.

145 A. P. Bassett, S. W. Magennis, P. B. Glover, D. J. Lewis, N. Spencer, S. Parsons, R. M. Williams, L. De Cola and Z. Pikramenou, *J. Am. Chem. Soc.*, 2004, **126**, 9413.

146 J. B. Coldwell, C. E. Felton, L. P. Harding, R. Moon, S. J. A. Pope and C. R. Rice, *Chem. Commun.*, 2006, 5048.

147 Y. V. Korovin, N. V. Rusakova, Y. A. Popkov and V. P. Dotsenko, *J. Appl. Spectrosc.*, 2002, **69**, 841.

148 R. F. Ziessel, G. Ulrich, L. Charbonnière, D. Imbert, R. Scopelliti and J.-C. G. Bünzli, *Chem. - Eur. J.*, 2006, **12**, 5060.

149 S. Comby, D. Imbert, A.-S. Chauvin and J.-C. G. Bünzli, *Inorg. Chem.*, 2006, **45**, 732.

150 F. Caillé, C. S. Bonnet, F. Buron, S. Villette, L. Helm, S. Petoud, F. Suzenet and É. Tóth, *Inorg. Chem.*, 2012, **51**, 2522.

151 A. Nonat, D. Imbert, J. Pécaut, M. Giraud and M. Mazzanti, *Inorg. Chem.*, 2009, **48**, 4207.

152 W.-K. Wong, X. Zhu and W.-Y. Wong, *Coord. Chem. Rev.*, 2007, **251**, 2386.

153 T. Zhang, X. Zhu, W.-K. Wong, H.-L. Tam and W.-Y. Wong, *Chem.- Eur. J.*, 2013, **19**, 738.

154 G.-L. Law, T. A. Pham, J. Xu and K. N. Raymond, *Angew. Chem. Int. Ed.*, 2012, **51**, 2371.

155 N. M. Shavaleev, G. Accorsi, D. Virgili, Z. R. Bell, T. Lazarides, G. Calogero, N. Armaroli and M. D. Ward, *Inorg. Chem.*, 2005, **44**, 61.

156 S. Torelli, D. Imbert, M. Cantuel, G. Bernardinelli, S. Delahaye, A. Hauser, J.-C. G. Bünzli and C. Piguet, *Chem. - Eur. J.*, 2005, **11**, 3228.

157 a) A. M. Nonat, S. J. Quinn and T. Gunnlaugsson, *Inorg. Chem.*, 2009, **48**, 4646. b) L.J. Charbonnière, S. Faulkner, C. Platas-Iglesias, M. Regueiro-Figueroa, A. Nonat, T. Rodriguez-Blas, A. de Blas, W.S. Perry, M. Tropiano, *Dalton Trans.* **2013**, *42*, 3667.

158 P. B. Glover, A. P. Bassett, P. Nockemann, B. M. Kariuki, R. Van Deun and Z. Pikramenou, *Chem. - Eur. J.*, 2007, **13**, 6308.

159 G. A. Hebbink, D. N. Reinhoudt and F. C. J. M. van Veggel, *Eur. J. Org. Chem.*, **2001**, 4101.

160 C. Doffek, N. Alzakhem, M. Molon and M. Seitz, *Inorg. Chem.* **2012**, *51*, 4539.

161 J. Wahsner and M. Seitz, *Inorg. Chem.*, 2013, **52**, 13301.

162 A.-S. Chauvin, S. Comby, B. Song, C. D. B. Vandevyver and J.-C. G. Bünzli, *Chem. - Eur. J.*, 2008, **14**, 1726.

163 M. Elhabiri, J. Hamacek, N. Humbert, J.-C. G. Bünzli and A.-M. Albrecht-Gary, *New J. Chem.*, 2004, **28**, 1096.

164 J.-C. G. Bünzli, *Interface Focus*, 2013, **3**, 20130032.

165 T. Zhang, X. Zhu, C.C.W. Cheng, W.-M. Kwok, H.-L. Tam, J. Hao, D.W.J. Kwong, W.-K. Wong, and K.-L. Wong, *J. Am. Chem. Soc.* **2011**, *133*, 20120.

166 A. D'Aléo, A. Bourdolle, S. Brustlein, T. Fauquier, A. Grichine, A. Duperray, P. L. Baldeck, C. Andraud, S.

Brasselet and O. Maury, *Angew. Chem. Int. Ed.*, 2012, **51**, 6622.

167 A. D'Aléo, A. Picot, A. Beeby, J. A. Gareth Williams, B. Le Guennic, C. Andraud and O. Maury, *Inorg. Chem.*, 2008, **47**, 10258.

168 A. Foucault-Collet, K. A. Gogick, K. A. White, S. Villette, A. Pallier, G. Collet, C. Kieda, T. Li, S. J. Geib, N. L. Rosi and S. Petoud, *Proc. Natl. Acad. Sci.*, 2013, **110**, 17199.

169 K. A. White, D. A. Chengelis, M. Zeller, S. J. Geib, J. Szakos, S. Petoud and N. L. Rosi, *Chem. Commun.*, 2009, 4506.

170 Y. Liu, L. Sun, J. Liu, Y.-X. Peng, X. Ge, L. Shi and W. Huang, *Dalton Trans.*, 2015, **44**, 237.

171 Q.-Q. Liu, J. Geng, X.-X. Wang, K.-H. Gu, W. Huang and Y.-X. Zheng, *Polyhedron*, 2013, **59**, 52.

172 Z. Liao, M. Tropiano, K. Mantulnikovs, S. Faulkner, T. Vosch and T. J. Sørensen, *Chem. Commun.*, 2015, **51**, 2372.

173 E. Debroye, and T.N. Parac-Vogt, *Chem. Soc. Rev.* **2014**, *43*, 8178.

174 K. Hanaoka, *Chem. Pharm. Bull.* 2010, 58, 1283.

175 C. Sun, G. Pratx, C.M. Carpenter, H. Liu, Z. Cheng, S.S. Gambhir, and L. Xing *Adv. Mater.* **2011**, *23*, H195.

176 M.A. Lewis, V.D. Kodibagkar, O.K. Öz, and R.P. Mason *Opt. Lett.* **2010**, *35*, 3889.

177 L. Aboshyan-Sorgho, C. Besnard, P. Pattison, K.R. Kittilstved, A. Aebischer, J.-C.G. Bünzli, A. Hauser, and C. Piguet, *Angew. Chem. Int. Ed.* **2011**, *50*, 4108.

178 D. Zare, Y. Suffren, L. Guénée, S.V. Eliseeva, H. Nozary, L. Aboshyan-Sorgho, S. Petoud, A. Hauser, and C. Piguet, *Dalton Trans.* **2015**, *44*, 2529.

179 O.A. Blackburn, M. Tropiano, T.J. Sørensen, T. Thom, A. Beeby, L.M. Bushby, D. Parker, L.S. Natrajan, and S. Faulkner, *Phys. Chem. Chem. Phys.* **2012**, *14*, 13378.

180 I. Hyppanen, S. Lahtinen, T. Aaritalo, J. Makela, J. Kankare, and T. Soukka, T. *ACS Photonics* **2014**, *1*, 394.

181 A. Nonat, C.F. Chan, T. Liu, C. Platas-Iglesias, Z. Liu, W.-T. Wong, W.-K. Wong, K.-L. Wong, and L.J. Charbonnière, submitted for publication.

182 T. Liu, A. Nonat, M. Beyler, M. Regueiro-Figueroa, K. Nchimi Nono, O. Jeannin, F. Camerel, F. Debaene, S. Cianférani-Sanglier, R. Tripier, C. Platas-Iglesias, and L.J. Charbonnière, *Angew. Chem. Int. Ed.* **2014**, *53*, 7259.